Fung Engineering Capstone
Mechanical Engineering

Vanguard Space Gloves

Research and prototyping an E.V.A glove intended for future mars expeditions that can preserve the functionality of a user's hand while minimizing injuries and discomfort

Submitted by:

Controls Engineer	Fu-hsiang Chang
Controls Engineer	Minglong Li
Product Design Engineer	Yuting Zhan
Thermal & Simulation Engineer	Thomas Chengattu

Under the Guidance of
Lawrence Kuznetz & Boris Rubinsky

University of California, Berkeley
In Partial Fulfillment Of The Requirements For
A Master of Engineering degree
Spring 2018

FUNG INSTITUTE
for ENGINEERING LEADERSHIP
UC BERKELEY COLLEGE OF ENGINEERING

Team Member Authorization Page

FUNG INSTITUTE CAPSTONE

We the team at Vanguard aspire to build martian space glove, capable to handle the grueling constraints of extraterrestrial travel and exploration. As graduate students in UC Berkeley's M.Eng program, we will be using the resources and our relative concentrations in our respective fields to work in a stimulating and collaborative environment. Each member of the Vanguard team has contributed to, and reviewed this final report in its entirety. Members all agree with its contents and authorize its authenticity.

Table 1: The Vangaurd Group - Contribution and Interests

Stanley Chang is a control engineer responsible for developing the controls algorithm of the robotic assist device. See section 3.3. This system will play an integral part of future astronauts being able to do work in a low pressure environment. He will be working closely with Minglong Li.

Role: Controls Engineer: _____

Minglong Li is a control engineer who will develop the sensory feedback system that will be used to collect data on the astronaut's physiology while monitoring the outside conditions to manage the robotic assist. See section 3.3. He is also in charge of developing the CAD model & 3D printing the prototypes. He will be working closely with Stanley Chang.

Role: Controls Engineer: _____

Yuki Zhan is a product designer who will build the first and subsequent revisions of the EMU glove CAD Design with traditional CAD software such as Fusion 360 and Solidworks and lead it to manufacturing. Along with the glove design, she will also be responsible for the locking mechanism. See section 3.1.

Role: Product Design Engineer: _____

Thomas Chengattu is responsible for creating a heat transfer model that can adequately simulate EMU conditions on Mars, in order to choose the material properties for the required fabrics. See section 3.2. He will also act as team project manager, helping to make the group follow a strict time line.

Role: Thermal & Simulation Engineer _____

April 30, 2018

Acknowledgements

Special thanks to our advisors, Dr. Lawrence Kuznetz (Dr. K) & Dr. Boris Rubinsky, and our GSI, Noah Bonnheim, for your help and support for this project. For the many people we interviewed and for other professors that helped us along the way.

Executive Summary

The Vanguard team looks to build an E.V.A. glove subsystem, capable for use on Mars. These gloves will preserve the functionality of a user's hand while minimizing injuries and discomfort involved with using gloves in space. We aim to use a robotic assist systems, and better ventilation to prevent finger injuries for next generation Martian space suits.

Mission Statement:

"Developing a space glove for future mars expeditions that can preserve the functionality of a user's hand while minimizing injuries and discomfort"

Value Proposition:

"The pursuit of understanding mars comes down to how we can make it home. To touch. To feel. To make mars human. The idea of a fully immersive environment is what compels us to make gloves that feel like they don't exist."

Contents

List of Figures

List of Tables

This page is intentionally left blank

Part 1

Introduction

We the team at Vanguard aspire to build Martian space glove, capable to handle the grueling constraints of extraterrestrial travel and exploration. As graduate students in UC Berkeley M.Eng program, we will be using the resources, and our relative concentrations in our respective fields, to work in a stimulating and collaborative environment. Team Vanguard's primary focus will be ensuring the capability of a novel, functional, space suit glove capable for use on future Martian Extravehicular Mobility Unit (EMU) suits. Thus we aim to build a design that can preserve the functionality of a user's hand while minimizing the injuries and the discomfort involved with using gloves in space. The design must allow the user to participate in any extra-vehicular activity (EVA), specifically suited for mars, while also preserving the full functionality of the user's hand. The design process will be iterative, and the final prototype will be manufactured in an ergonomic and lean way to reduce costs. The design must also be allow all further suit components to fit well into the suit, and must allow for seamless system integration to some degree of freedom. The following section briefly outlines the problem space.

Martian exploration increasingly becoming a reality

Traveling to Mars poses many challenges in comparison to those faced while in orbit or on the moon. For one, the Martian gravity puts a significant weight restriction on the final design of the space suit. Having a suit that can sustain life, while being downsized, is a key challenge in space suit development for Mars. Along with the functional requirements of the suit, general comfort and non-restrictiveness dictate the quality of the work astronauts will be able to conduct. Thus, finding weight reducing elements while keeping the comfort paramount, will play an important challenge to space suit development.

The current space industry platform is relatively nascent, however space is teeming with opportunity and is ripe for ethically uncomplicated exploitation. Some have predicted that it will be the first industry to produce self-made trillionaires [1]. The privatization of space and the establishment of private outposts far from the watchful eye of mother Earth might prove to be one of history's most important developments [1]. Along with notable leaders such as SpaceX and NASA, a platform of new space-related startups have been trending recently. Startups such as Planetary Resources, a company looking to mine asteroids for water as jet propellant, or Made in Space, a company looking to utilize lack-of-gravity manu-

facturing, show the broad nature of economic possibility in space. As such, space clothing is an equally appealing platform.

Investors have also begun taking space much more seriously. Based on CBInsight data presented below, global funding for space related technology has been on a noticeable climb for the past few year [2], see figure 1.1(b), and the number of startups in space related industry has been growing with increasing popularity [3], see figure 1.1(a). These trends indicate a F.O.M.O culture for investors; space is simply becoming an attractive business. Along with these trends we we believe the noticeable uptick in investor activity in this area is fueled by the lack of government regulations and a growing interest in space from the public.

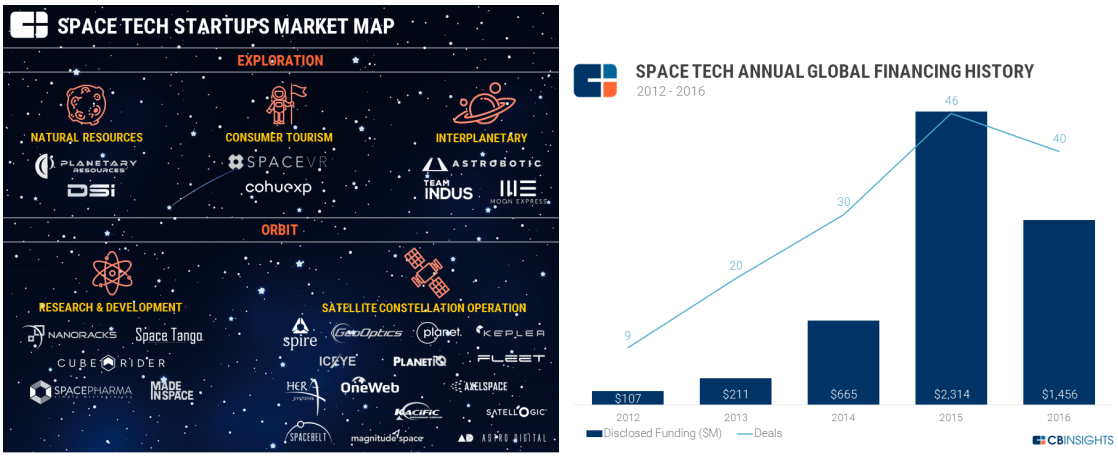

(a) Space Tech Startups [2] **(b)** Space Tech Financing History [3]

Figure 1.1: Space Startup Market

As seen above, VCs are beginning to look into space related industries with much more opportunity than skepticism. Our assumptions is that with a growing new business ecosystem, and a breath of new commodities needed to develop space, properly led businesses are taking similar risks as Vanguard. Using these trends to our favor, along with NASA's, SpaceX's [4], and potentially even Lockheed Martin's [5] interests in mars colonization, we believe our business venture has a potential to get funding as we develop the technology.

■ Human activity on mars limited by Spacesuit Design

Although the journey to Mars brings its own complications and challenges, there exists significant challenges of making humans live and work on Mars. One of the biggest one would be the quality of the Mars Suit. "A good space suit is like a personal space ship: It must keep you alive but also help you live." [6] Addressing critical life-supporting, and Martian specific commodities also become an important issue when dealing with Martian space travel. Exploration and protection are two main desires for spacesuit construction. Although sound in theory, the Martian environment is a big limiting factor to what humans can and can't accomplish. "We need to able to bend down on one knee to collect a rock sample, or use our uniquely opposable thumbs to grip a tool and make a repair"

[6]. Making the space suit comfortable while making sure it can handle the rigors of mars are two main factor in the design procession.

Current problems in E.V.A Spacesuit design

Along with the high degree of freedom needed, the martian environment itself is the greatest challenge while designing for space suits. Some of the major tasks required for environmental protection include radiation prevention, temperature and pressure regulation. Damage issue report also showed that hand and especially fingers accounted for the majority of problems [7]. In Gerhardt's article about injuries due to EVA operations, it is stated that these injuries happen "during both training and flight [7]". The reason behind that is the fact that the whole suit is pressurized, thus, fingers are constantly fighting the pressure to deform the gloves, and therefore, perform tasks. The constant pressure environment has the tendency of exerting excess forces that the human hands are not used to opposing causing injuries

Another difficulty with designing a suit for Mars colonization is the weight requirement of the suit. In the context of Mars colonization, the suit has to be used the whole day as opposed to a traditional EVA suit that is designed for only a few hours of use per day. Current EVA suit weighs around 220 pounds on earth, and a trained person can operate normally and perform delicate tasks with a load of only 50 pounds [8]. Therefore, it is critical to design a space suit with significant less weight than the current design. And more specifically to the glove part, the goal is to maintain the weight of current design and to reduce the requirement for support from the suit.

Part 2

Design Procedures & Requirements

When we first began the project, we tried to identify the biggest challenges surrounding current spacesuits. This first step helped connect the broad requirements of the entire space suit to the specific requirements of the glove. Gradually the scope has narrowed down to a focus for (EVA) gloves. Unlike arms, legs or the torso components of the suit, the hands of human beings have the highest degree of freedom [9]. Thus, the amount of dexterity available will greatly dictate how efficiently tasks can get done and how astronauts will be able to interact with their surroundings. Current space gloves are uncomfortable after long periods of work and cause trauma to the fingers, sometimes even loss of fingernails. Thus, finding ways to reduce the weight of spacesuit components, specifically the gloves, while keeping them comfortable to wear for a full work day, will be an important challenges to face.

The following section will outline how team Vanguard selected key design parameters for focus, and will briefly describe the iterative design process used in building the prototypes.

Human Centered Design process used to understand the needs of future Martian explorers

The design quality and limitations of the Mars Suit would influence the success of a manned mission to Mars. The Human-Centered-Design process was used to understand key requirements needed for an effective glove design that is "human-usable".

2.1.1 Glove design process focused on rapid idea generation and prioritizing certain requirements

The human centered design process (HCD) has been characterized by repeated cycles of broad idea generation followed by narrowing down and focused development. Over the course of our first four months, this cycle occurred in the areas of stakeholder analysis, needs selection and product design. Since no Martians currently exist, we needed to get creative on how to gather the right types of information.

We were also able to gather some of the limitations of the current space suit gloves. Using brainstorming methods learned in Human-Centered Design we generated a large number of potential concepts that could be incorporated into the gloves.

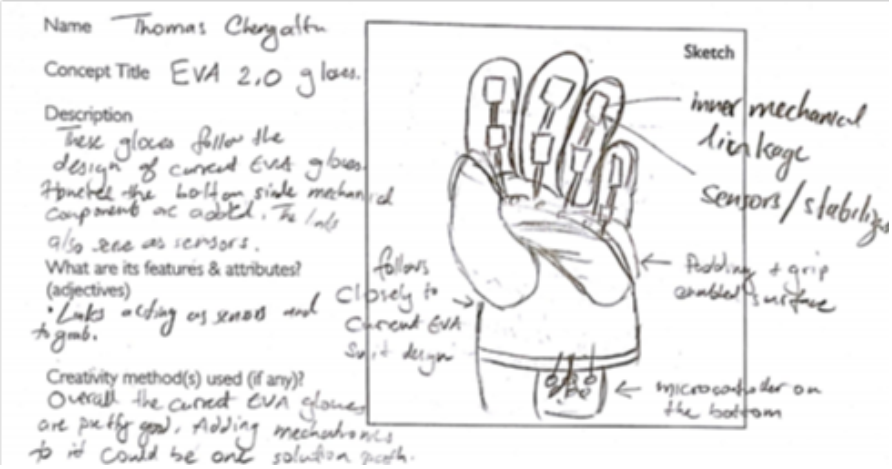

Figure 2.1: Initial Sketches

Figure 2.1 illustrates one such design. Using some of the methods learned from the design exchange, our members were able to draw up many different space glove concepts. These drawings helped identify needs and helped to understand how certain features could be incorporated. The relatively large list of concepts was then parsed down substantially through a selective process, incorporating design prioritization and feasibility determination. Lastly, we incorporated and tested various features during our prototyping efforts to learn more about pressurization and comfort while in use. The following section goes further into detail.

The next section describes the research conducted using various HCD Methods. These methods are underlined in the next section.

2.1.2 Human centered research methodologies were used to understand future user needs

For our initial needs assessment, we started with interviewing analogous users because the true end user, a Martian astronaut, does not yet exist. We reached out to professionals that dealt with extreme environments, including Antarctic ice-core drillers, wilderness fire helicopter pilots, construction workers, firefighters and race car drivers. We also conducted secondary research from a variety of resources including movies about Martian travel and NASA articles. 1:1 interviews and open card sort provided us with the opportunity to address issues and needs found in gloves used in various activities on earth. Based on feedback from these interviewees we conducted an open card sort and found our major topics of interest to be **dexterity, comfort and protection**.

Once our needs were found from the interview process, we used an empathy map to construct a fictional character who would one day use our space suit gloves. Backed with secondary research from "The Martian" we were able to give our persona a mix of personality, traits, and roles for their Martian life. We found

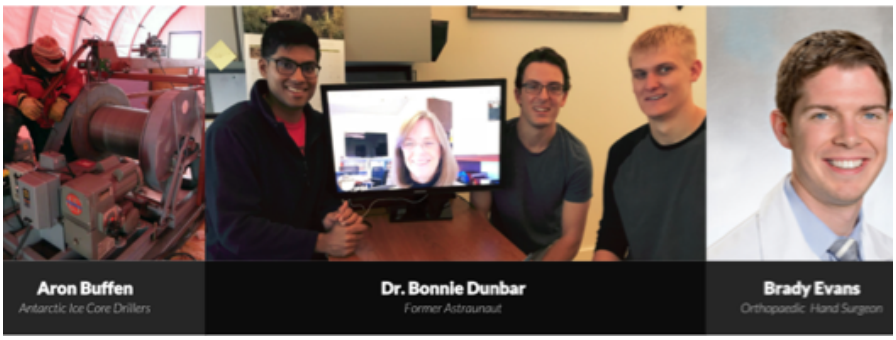

Figure 2.2: Interviewees

that our Martian would undergo conditions best matched by the arctic worker who we interviewed.

A "why ladder" design method was then applied to our fictional Martian character, backed with knowledge from our 1:1 interviews. Both design methods lead us to the discovery that the "one size fits all" model for gloves would be severely limiting. Some users would have increasing discomfort due to fitting issues or experience the dexterity degradation that is caused due to improper fit. Furthermore, we believed that improper fit may also not provide adequate environmental protection to the user, which on a foreign planet can mean life or death.

Thus, using the learnings from our interviews, building a persona and using abductive reasoning, we began to work on a glove design that would fit the needs of a future Martian user.

At this point, we had a much better idea of our purpose and were able to develop a value proposition: *"The pursuit of understanding Mars comes down to how we can make it home. To touch. To feel. To make Mars human. The idea of a fully immersed environment is what compels us to make gloves that feel like they don't exist."* This value proposition gave our project an objective for our prototype. Furthermore, a stakeholder analysis helped us define what our end goals for success will be, and the frequency of interaction needed between key individuals. By balancing faculty influence, and our knowledge of needs and requirements from outside sources, we were able to conclude who we need to consistently inform and work with for this project.

Now that the needs had been identified, and our overall success factors and audience determined, we started the concept generation phase. To develop a robust list of potential concepts for our design we used several idea formation methods starting with individual brainstorming. Then, together, we used a modified 6-3-5 technique. This method was very useful in generating a lot of concepts quickly, but what we found was there was a tendency to have fairly similar products after the first couple of passes. As novice designers, we hit the point where novel concept generation began to be difficult. Regardless we kept at it for several weeks.

Based on the initial list of concepts, our team began narrowing down future concepts and identifying key needs. We used internal surveys and Borda voting to develop a list of prioritized needs. The greatest needs for our end user would be dexterity, comfort and temperature and pressure regulation. Being light weight and aesthetically-pleasing were ranked to be the lowest needs.

2.1.3 Use of rapid prototyping techniques to understand challenges involved in EMU gloves

The first prototype that was built looked into creating a pressure layer. The pressure glove was created to recreate the comfort level a user may feel as a result of feeling a pressure delta. The overall prototype was built using a rubber glove to hold air, along with a stiff motorcycle glove to hold the pressure layer. Figure 2.1.3 shows the sequence of steps involved in this build.

(a) Pressure Layer **(b)** Filling Pressure **(c)** Prototype 1

Figure 2.3: Low-Fidelity Prototyping : Phase 1 - Pressure Layer

We immediately learned that pressurized gloves bring severe limitations to the user's overall dexterity. Furthermore having it pressurized, even slightly over $1atm$, caused extreme irritation to the skin. The takeaways from this prototyping was understanding the impact of dexterity with a stiff glove.

Next we understood how tricky it it could be to control the pressure layer. During user testing, the air bubbled in a nonuniform manner, mainly spreading in the palm region. We noticed that the top of one's hand, including the knuckles, had very little ballooning effects. These were most likely due to stiffer materials being used in the top of the glove.

Lastly we noticed that fine motor skills were almost obsolete. The user had to use their fingertips more in order to proceed to any task. Specifically during user testing, we received feedback that users desired for claws or more flexible fingers

(a) Stiffer Glove **(b)** Metal plate on stiff glove

Figure 2.4: Low-Fidelity Prototyping : Phase 2 - Controlling the ballooning effect using a stiffer glove and a metal plate.

Our next low-fidelity prototype looked into combating the ballooning issue, and understanding how to fix dexterity in the "palmer" area.As seen in figure 2.4b, the metal plate was used to combat the effects of the ballooning. Essentially this mechanism forced the air into the upper region of the glove.

Deriving critical design requirements for Martian space gloves

Based on the human centered process, and further inquiry into the problem space, team Vanguard was able to narrow down the scope of the project to the EMU glove. Within this problem space, the focus was on three specific requirements: increased dexterity, better comfort and protection from finger-nail related injuries.

Dexterity was defined as the ability to actually do a particular task well using one's hand - this included picking up objects to maneuvering one's finger. This requirement was drawn from the experience of the Antarctic ice-core driller. He had explained that the gloves they use often prevented them from moving their fingers, especially for precision-related tasks. As a result, he and his colleagues often had to temporarily remove the glove for such tasks. On mars, these actions wont be possible. Thus enabling a high degree of freedom will a requirement.

The overall **comfort** while a user moves his/her finger will determine the effectiveness of the EMU glove. The end user will be required to work for roughly an 8 hour shift everyday while on Mars. This requirement was pulled from mars suit problem statement. Since astronauts are required to work for a "typical work day" we need these gloves to prevent any frustration as a result of daily use. Based on the ice-core driller we interviewed, we also learned that gloves were often switched periodically, so that the extra pair remains warm. Furthermore future gloves should also come with a variety of sizes to fit for users with different hands.

Functionality will play a vital role as well. Since these gloves are needed to be used in Mars, it needs to provide adequate environmental protection and pressure regulation. Although Mars has many environmental constraints, for the duration of the project we focused on temperature and pressure regulation - maintaining pressure differences without the hands becoming numb or too cold or hot. Another important functionality requirement stemmed from the most commonly cited issues for space gloves - fingernail related injuries [10]. Using the insight developed, and understanding the major concerns seen in the fingers, our team focused in on creating solutions for minimizing and preventing fingernail issues in future glove design.

Part 3

Technical Methodology

Based on the design requirements that were defined earlier, we realized we should focus on one major parameter to keep our technical report more focused. Therefore our technical section will focus on fingernail related injuries that occur in current EMU glove.

As we investigated the root causes of the problem, two potential reasons linking fingernail damage was found. One major issue is humidity accumulation in the fingers. Based on an interview with a former astronaut, we found that previous spacesuits were designed as closed system without appropriate air circulation or ventilation. Therefore, sweat accumulated fast and could not be removed adequately near extremities, such as fingers. As excessive moisture accumulated in the fingers, the keratin in fingernails became softer which lead to increased chances of fingernail damage. This damage is usually propagated as a result of the gripping and holding tasks . Furthermore, as astronauts fight the pressure delta that is inherently built in space suits, which are highly pressurized compared to vacuum of space, the weakened fingernails and repetitive hand-related tasks that fight pressure will cause nails to break or become damaged. Thus the weakened keratin structure and the repetitive loads on the fingernails from daily tasks are two of the major reasons for fingernail damages.

Based on these issues we found that two main approaches, if done in parallel, can help aide in dealing with one of the most common issues with space gloves. One - an open loop system designed to bring a steady stream of Martian air, at a protective distance away from the skin, could prove useful for ventilation purposes. This method's success hinged on the material properties being used to protect the skin against the air, and ways to control the open loop air system. However if both can be managed, the use of Martian air to carry evaporated waste water could help mitigate humidity. Furthermore, we noticed that the excessive forces required in gripping and holding tasks could also be assisted. The second solution involves using a robotic augmented system, which using sensors that captures the movement of the hand motion and peripheral environment, will control actuators that provide the extra force to help the hand. Thus this method will look to reduce the load that is being applied on the fingernail during repetitive tasks.

The technical report will begin by highlighting the "open loop system", and how it will work with the EMU glove. Then the report will discuss how moisture and temperature can be controlled to mitigate the effects of a moist fingernail environment. Lastly the report will discuss th effect of a robotic assist system

Designing an open loop system for Martian EMU Gloves

The research and design for Vanguard gloves are drawn from earlier work done by Professor. Lawrence Kuznetz, who chose an "open-loop system" for the whole Mars suit. One challenge in space suit design is keeping a pressurized system for the body. In deep space, the lack of atmosphere, or any molecules, means that the space suit has to be a closed system - bringing all the necessary functions required to survive in any condition. Unlike the traditional closed-loop system, in which the helmet and the torso are pressurized as one unit, the open-loop system isolates the helmet from the torso. Further, unlike the developing mechanical counter pressure system, which pressurizes the body mechanically using form-fitting garments, the open-loop system uses the Martian atmosphere (CO_2) to pressurize the body directly. Mars on the other hand, has an atmosphere full of CO_2, which have occupied 95.32% in Martian atmosphere. Additionally, Mars is much colder than Earth, because of the Mars' thin atmosphere and its greater distance from the sun, which is also another pain point for the Vanguard design [11].

One of the most important topics in Extravehicular Activity (EVA) space suit research is the gloves, which is one of the particular parts of the whole suit design. Astronauts have to perform various tasks in space by their hands, like gripping without plenty of extra effort, or with high dexterity and comfortability [12]. Additionally, prevention of fingernail delamination and other potential injuries of hand is also important for the whole design. The bulk and stiffness of the glove itself make it difficult for astronauts to perform their diverse daily tasks in space and on mars[13].

3.1.1 Benefit of the open loop system and how it works

Though the atmosphere of Mars is about 100 times thinner than Earth's, CO_2 have occupied 95.32% in Martian atmosphere, while it only contains 0.13% oxygen [13]. Thus unlike using a closed-loop approach seen traditionally for spacesuits, the Mars Suit will have the advantage of using the Martian atmosphere to create an open-loop pressurized system, using the CO_2 for pressurization. The primary benefit of this method is the significant downgrade in the complexity of the suit, and the benefits of weight reduction. Furthermore, with Martian atmosphere constantly flowing within the suit, we can use the air for ventilation purposes to tackle excessive moisture found in the fingernails. See the diagram 3.1,ventilating mars gas is between protective skin liner and pressure bladder, while the assistive system is attached the protective skin liner directly.

The open-loop system will only be possible for the torso-leg-hand-extremities section. The head will need a constant flow of oxygen and will be pressurized via a closed-loop system. Due to this design choice, the open-loop pressure will succumb down to 3.5 psi, which according to previous tests by NASA is a sufficient internal pressure for the suit if the wearer breathes pure oxygen[14].

Current EMU uses Oxygen to pressurize the whole body, while a puncture for the suit is a fatal disaster for the astronauts in the Space, which would result in

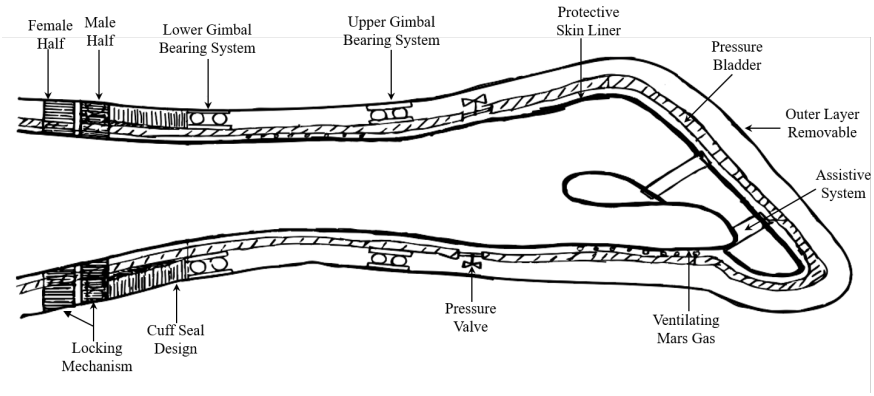

Figure 3.1: Open loop system of the Vanguard Glove

rapid decompression. As Parker and West's studies in 1973 have shown, astronauts only have 9 seconds of consciousness to save themselves. Even under normal operation conditions, more than 50 liters of oxygen would lose up per hour by the connection part of the whole suit. However, open loop system will allow the astronaut more time to reach safety in the case of depression and also minimize oxygen lose [15].

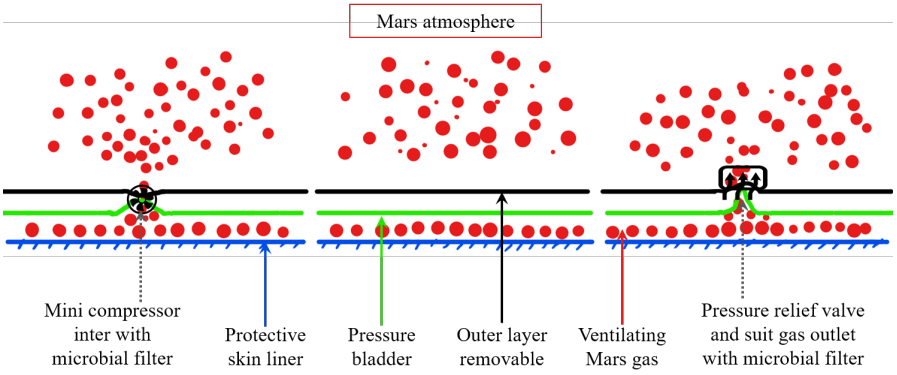

Figure 3.2: Layer specification of the open loop system

Generally, astronauts would wear thin fabric comfort gloves with knitted wristlets under EVA gloves. In the Vanguard gloves design, it includes three layers apart from comfort skin liner [16] (see the diagram above 3.2):

I. Ventilating Mars Gas: First layer, directly connect to the protective skin liner, used to maintain the pressurized environment of the gloves.

II. Pressure Bladder: Second layer, creating an impermeable barrier to carry all pressure with ventilating Mars gas inside and other man conducted loads during the operation.

III. Thermal-micrometeoroid garment (TMG) layer: Outer layer removable, to provide a barrier to keep thermal conditions and protest the space particles and other known or unknown radiations.

■ 3.1.2 Design challenges within open loop system

As mentioned previously, the separation between head and torso is the basis of the Mars Suit. CO_2 is the gas used to pressurize the torso and extremities, which

would greatly lower the consumption of oxygen and also extend the time of useful consciousness for the puncture from seconds to minutes or even hours.

Incorporating the open loop design with a specified pressure to our glove design will cause some challenges. For example, the tissue pressure felt on the body has a certain minimum threshold. If the exerted pressure on the tissue matches the blood pressure, then blood circulation can become compromised. Along with necessity of keeping the tissue maintained at a certain minimum pressure, the joints involved with the design need to have properly tightened seals that can control pressure while still allowing a hand to rotate [17]. It is imperative that solutions enable proper function while not limiting user mobility. For reasons of scope and resources, the pressure control for the open loop will be focused towards the cuff seal - disconnect design.

The disconnect will need to have a few design requirements. The pressure seal will be imperative to maintain a certain pressure value while providing ease of donning and doffing [18]. Being able to don and doff while allowing for the full freedom of hand-related motion will be an important emphasis on the human-centered design element of the Vanguard Gloves. The pressure seal component will also incorporate the use of light pressure bearing aimed at reducing the overall weight and enabling pronation-supination movements. Thus the four main design features included in the final concept prototype will include:

I. Easy donning and doffing cuff seal design

II. Male and female design with integrated ventilation channels

III. Low torque and low leakage glove-bearing disconnects

IV. Lightweight and low profile bearing design

■ 3.1.3 Relative design

Like traditional EMU spacesuit design, individual fingers and thumb will be separated in Vanguard gloves design, which will be molded as a hand covering sheath with rubberized fabric. The fabric layer will provide a restrained layer of the whole glove when the carbon dioxide is pressurized in the gloves, which also provide a good fit and better flexibility. In order to increase comfortability, current space gloves are molded to size from a cast of the real astronaut hand. Addition to that, restraint cable and also bladder projections at the finger joints also provide increased flexibility.

I. Easy donning and doffing cuff seal design

On average, Mars exerts only 6.1 millibars (0.087 psi) of surface pressure, which is about 0.6% of Earth's mean sea level pressure of 1.013 bars (14.69 psi).[19] As research has shown, human's respiratory and circulatory balance can be a problem when in such a low pressure environment. Current design pressure of the NASA EMU space suit is about 4.3 psi, which is 100% oxygen [19]. However, in Vanguard design, the pressurized gas would be carbon dioxide instead of oxygen.

Blood pressure would increase when ambient pressure increase. Hence, how to keep the tissue pressure matches with blood pressure is crucial for a proper blood circulation. For Vanguard potential future users, the ambient environment is Martian surface pressure, it would be a disaster for them if they don't have

a sufficiently high pressure for tissue, because the veins would be engorged with blood and the worst result is blood pooling. When the gloves want to connect with the torso, how to maintain a pressure seal at the joinder point while still allowing a hand to rotate and ease of donning and doffing increase the design difficulty.

When Vanguard gloves designed with open loop system, in order to prevent blood pooling and also keep ease of donning and doffing for the joinder point, when the hand are pressurized by the Martian CO_2 directly, the cuff seal design should be pressurized by an elastic material which supplies a mechanical counter pressure directly on the skin. In this way, the pressure exerted thereon lead the contact portion (shown in 3.3b) can move toward the longitude axis of the seal assembly or rotate with the axis of the seal assembly. When the gas pressure is increasing in the glove, pressure for the cuff seal is increasing which also enhances the pressure of contact potion on the wrist. When the gas pressure is decreasing in the glove, pressure for the cuff seal is also decreasing, so is the amount of pressure in the tissue. In this way, the gloves can be easily donning and doffing along with the pressure changing.

The following figures (3.3a,3.3b,3.4) depicts the cuff seal design, which is used for human's wrist.

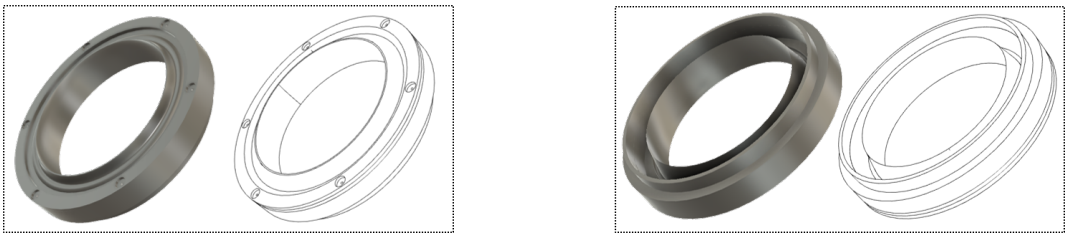

(a) Top View **(b)** Bottom View

Figure 3.3: Top and bottom views of cuff seal design

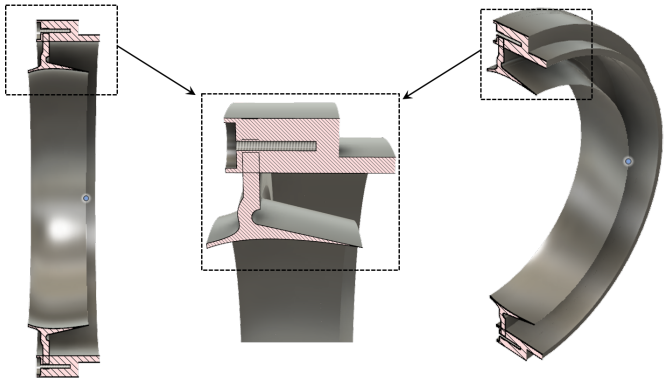

Figure 3.4: Section views of cuff seal design

II. Male and female design with integrated ventilation channels

Vanguard gloves will be joined with the torso sleeve by a rotatable metal interconnecting locking rings assembly (suit ring as female half —— figure 3.5 ring 1, glove ring as male part —— figure 3.5 ring 2) [20]. Suit ring comprises a locking ring on a housing to which is mounted a vent fitting. A pair of lock tabs and a lock button (not shown here but they should be in the ring 2) will be provided with the locking ring, the index marks will be used to align the suit ring with the glove ring. With the locking rings and index marks, the male and female part can be locked together in seal tight relationship to connect the Vanguard gloves with the torso sleeve, so is the connection of ventilation channel inside of the locking rings. The compressor in the torso will compress the Martian atmosphere and transport them into the open loop system of the torso. After the gloves joined with the sleeve, the pressure will also transport into the glove within the ventilation channel. Pressure relief valve adapted to open at a predetermined pressure (3.5 psi - 5 psi is a idea pressure range [14]) to automatically relieve the pressure within the suit when it becomes too high.

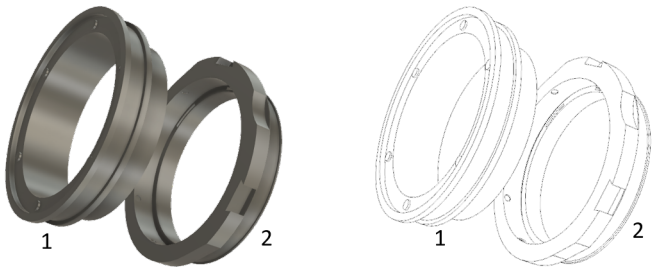

Figure 3.5: Perspective view of the disconnect design

III. Low torque and low leakage glove-bearing disconnects

Wrist motion will rotate with the good-design bearing and be followed in low-torque need. Enhanced rolling convolute wrist joint using two gimbal ring systems which are tightly integrated with the wrist soft-goods to reduce effort in a combination with lower torque wrist bearing [21]. The glove ring snaps into the suit ring, which contains bearing to permit rotation for added mobility in the hand area. In our design, when astronaut moves the rectangular-shaped tabs in one or two sliding to right or to the left, the glove-sleeve connection can be opened or locked easily.

Under normal operating conditions, the current EMU design will leak approximately more than 50 liters of oxygen per eight-hour-operation [15]. These losses of oxygen largely limit the use of entire spacesuit in exploration in space. The benefit of Vanguard's design is the oxygen will be replaced by carbon dioxide, which is compressed the Martian atmosphere directly by the compressor in the torso. It can greatly reduces the threat of puncture and abnormal oxygen leakage to astronauts. Helmet-torso separating system also greatly reduces oxygen consumption in the extravehicular activities, which can extend the tasks duration into a longer one.

Although it does not completely eliminate the effects of air leaks at the locking connection, effective reduction of leaks is also important throughout the design. O-ring seal will be used in the locking rings to prevent the pressurized gas lose from the glove.

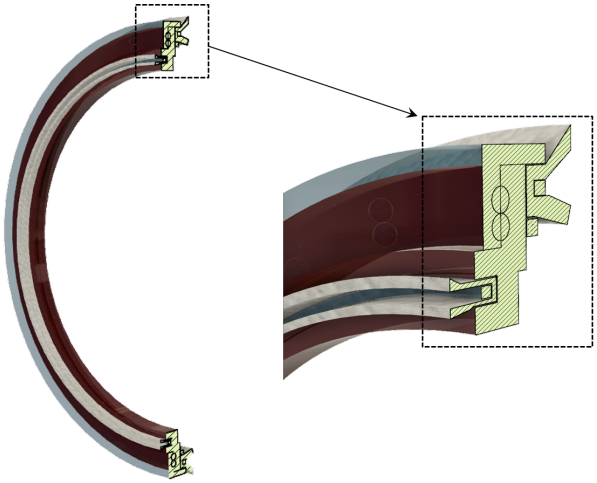

Figure 3.6: Section view of bearing design

IV. Light weight and low profile bearing design

Martian environment exerts a lot of challenges on Mars suit design, like micro-vacuum atmosphere, wide temperature fluctuations, and physical hazards (like dust storm, micrometeoroids, and radiation). Especially the Vanguard gloves is designed for people who will conduct a long-run exploration mission in the Mars, making the material choices become important. One crucial part for the gloves even for the whole suit is the pressure bearing design, which can facilitate the range of motion that can affect the astronaut's surface activities performing.

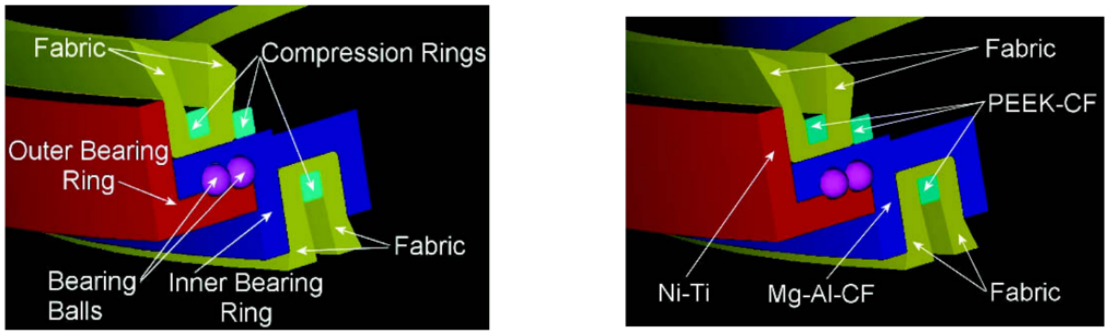

(a) Bearing apparatus [23] **(b)** Bearing Material Selection [23]

Figure 3.7: Bearing design and material choices [23]

In order to improve the range of motion for Mars suit, the pressure bearing should satisfy three main requirements: high motion flexibility, air sealing,

and lightweight. [22] In order to achieve that, the materials should possess high abrasive resistance, low friction coefficient, high elasticity modulus and high size stability [22]. In J. L Marcy's research, a bearing for Mars suit should include (see figure 3.7a): outer ring, inner ring and compression ring [22]. Corresponding materials used are (see figure 3.7b): Ni-Ti Shape Memory Alloy for outer ring, Mg-CF for inner ring, and Polyetheretherketone + 60% carbon fiber for compression ring [22].

V. Other general designs for gloves system

Additionally, there are several specific design features will be included in the gloves general design in concert with the open loop system (shown in figure 3.8): heaters in the fingertips, light bulbs located the back of gloves, fabric joints for all fingers, palm's retention device to preclude pressurized ballooning of the glove, a custom formed and high strength palm bar to conformal fit and allowed higher flexibility, a segmented palm plate to make the palm of the pressurized glove match the natural shape of the hand, etc. Those affiliated design will make the gloves more conformal with improved mobility joints that could function well at a high operation pressure.

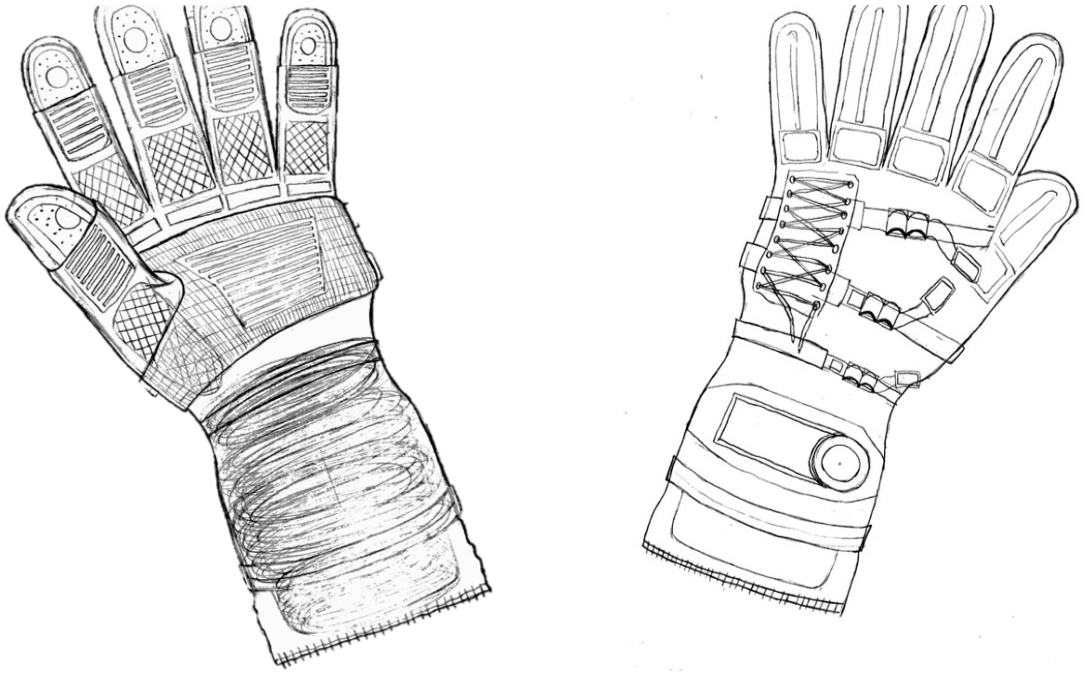

(a) Front view **(b)** Back view

Figure 3.8: Appearance concept design of Vanguard gloves

Modeling heat and moisture transport for an ideal Martian EMU

Fingernail injuries in spacesuits have been linked to an increased accumulation of sweat near the finger. This accumulation of moisture occurs primarily due to the current design of the suit ventilation systems. Notice the ventilation system diagram below, 3.9a . The feed oxygen begins circulating from the tank located near the back of the extravehicular mobility unit (EMU), and is dispersed in the head area first, before traveling downward to the extremities. As the oxygen travels to the extremities, it becomes much more humid - picking up all the excess moisture from the body. This excess water is slowly carried off to the hands and feet, before exiting via the labeled "out-tube". Thus the current ventilation system has the negative effect of transporting excess sweat to the user's extremities.

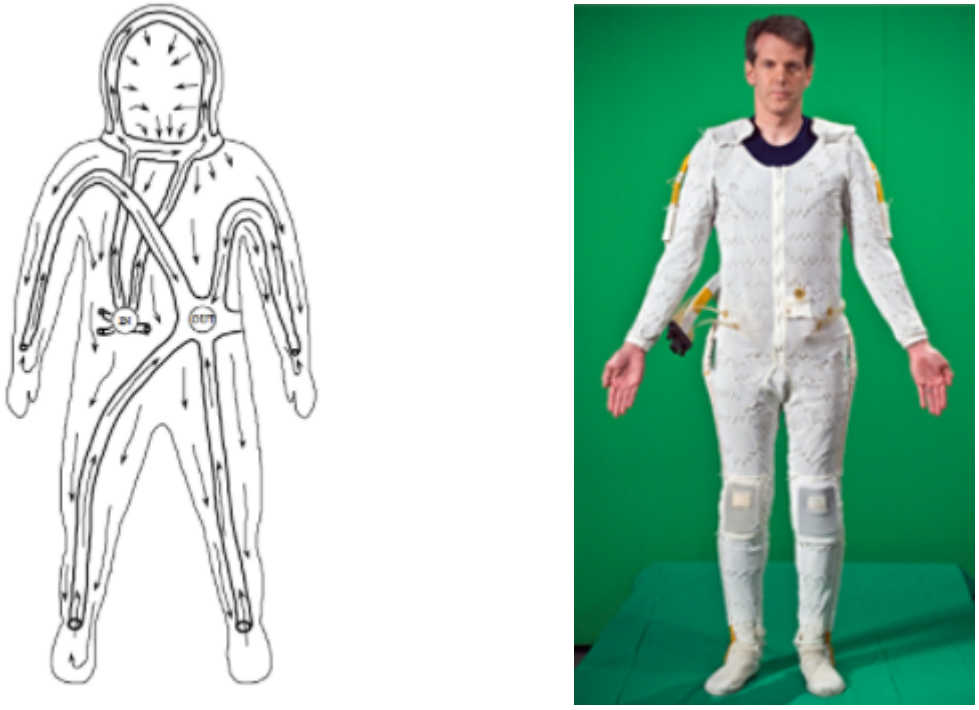

(a) Ventilation System [26] **(b)** Liquid Cooled Garment [25]

Figure 3.9: Images describing how moisture is evacuated in current suits (*a. Ventilation System*) and how body is cooled (*b. Liquid Cooled Garment)*

According to the study conducted by Lubach et al [24] , "frequent alternating periods of hydration and drying increase the incidence of brittle nails, particularly in women". In order to decrease the damaging effects to fingernails, it is critical to manage the suit ventilation process, and adequately remove all the excess sweat.

Using the previously mentioned "open-loop" system, in section 3.1, the team hopes that the flow of fresh CO_2 in the torso-leg-hand-extremities area will help to remove the moisture from the body into the environment. The study conducted in this section, will elaborate on these assumptions to understand exactly how much mass transfer is possible in a mars-suit environment.

Furthermore, an added benefit seen from the changes in the ventilation system is the possibility of achieving major weight reduction. Liquid cooled garments (LCG), see figure 3.9b, act as heat exchangers within current spacesuit - pumping water through narrow tubes near the skin. The vents in the garment draw sweat away from the astronaut's body which help in the ventilation and recycling of sweat. Oxygen is pulled in at the wrists and ankles to help with circulation within the spacesuit. Although the system acts well to maintain homeostasis, the major drawback of the design is the complexity of the system and the weight involved - the excess weight is due to having to store water, and having on-board chillers and heat-exchanging mechanisms.

Thus by incorporating an open loop system, the team hopes to address the challenges seen with adequately removing sweat and get the added benefit of removing excessive heat from the skin surface.

3.2.1 Requirements for open loop system using forced convection and evaporative cooling to provide EMU comfort

The open-loop system was originally planned as a method of pressurizing the EMU. However, one of the side benefit of this system is the ability to have recirculating CO_2. The inlet CO_2 is dry and cold, allowing it to pick up and remove heat, perspiration and contaminants from the astronaut as the air circulates across the body before exiting at the relief valve. The image below shows the a control-volume representation of the skin-fabric-ventilation system.

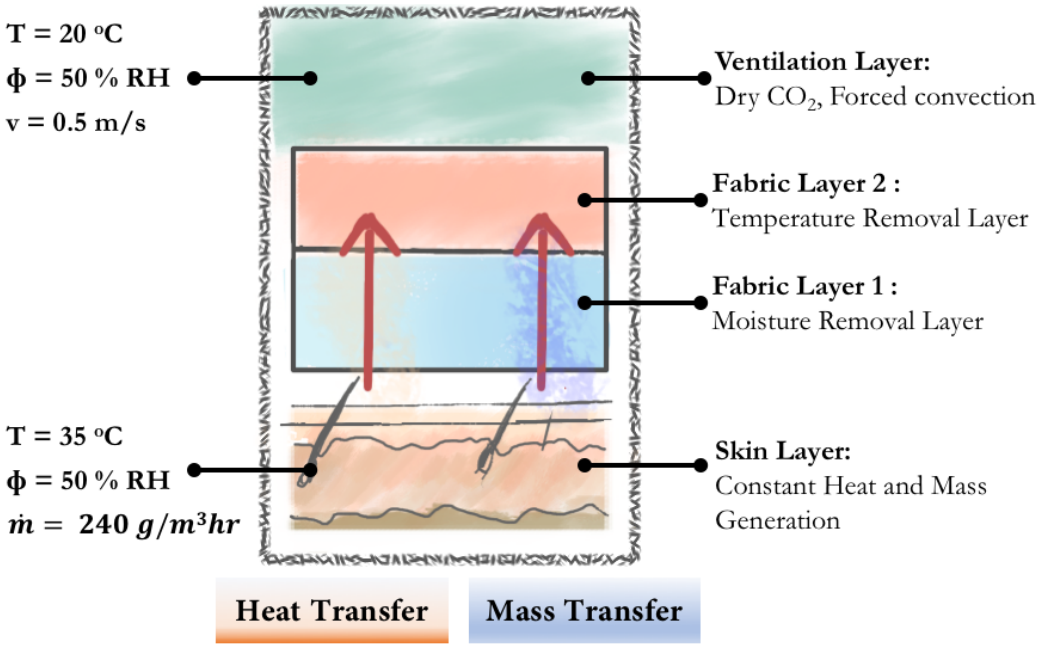

Figure 3.10: Schematic diagram of a multilayer fabric facing the user skin and of the surrounding open-loop environment conditions

The first requirement is enabling sufficient heat transfer from a working state. We will be using a combination of convective an evaporative cooling to cool the

user's body temperature to a comfortable value. The heat transfer method involved in the "open-loop" ventilation system must be capable of matching the LCG's cooling abilities. Evaporative-based heat transfer capability of our open loop membrane design should far exceed the 900 BTU/hr [27] , roughly 263.763 Watts, convective/evaporative capacity of today's EMU and should equal or exceed the 2000 BTU/hr [27] , roughly 586.14 Watts, capability of current LCG. It is critical that the system be able to handle metabolic rates that may peak at 2000 BTU [27] or more, as this represents peak work rate for individual during an "exercise" state.

The secondary goal is to provide adequate mass transfer of sweat, through one-directional hydrophilic membranes. These material ought to be able to promote sorption and carry water molecules to the surface of the material. The fabric used must be capable of transporting all the sweat within 10 minutes of a user's worked state.

We hypothesize that adding an "open-loop" mechanism will achieve sufficient moisture removal, and help regulate temperature via evaporative cooling and convective cooling from the ventilation pocket. If successful, we will be able to regulate cooling, mass-transfer and weight reduction for the suit. The results will be justified using Dr.Kuznetz's 41-Node Man Software, to validate the accuracy of the results along with relevant literature

3.2.2 Formulation of the heat and mass transfer model relating sweating mechanism during an active state while using an EMU

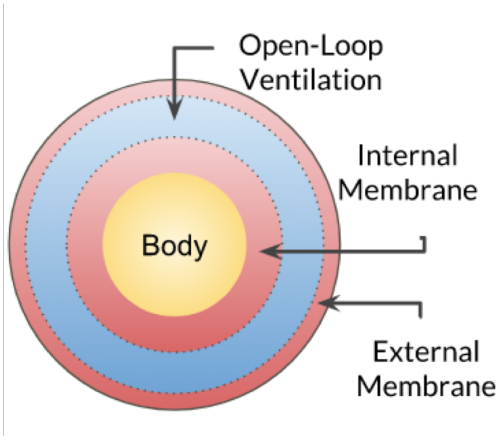

Figure 3.11: Glove cross-section highlighting the locations of the inner/outer membrane

The overall study looked to use numerical simulations to analyze the effect of several fabric properties (affinity with water, coefficient of water diffusion in the fabric, thermal conductivity, density, and specific heat) and textiles specific characteristics (outer surface emissivity, tortuosity, and fraction of fiber) on the heat and mass transfer across a textile assembly. We assume that the final Martian EMU will be composed of many user protective layers to handle comfort, protection and functionality. This study will exclusively focus on the internal membrane, see figure 3.11, which we assumed to be made of a blend of fabrics. The chosen fabric must contain properties such that the diffusivity of water vapor in the material must remain high, while allowing for sufficient heat conduction. Thus the internal membrane is assumed to be made of a two-layer fabric component.

The works of S.F. Neves [28], P. Chitrphiromsri [29] and Gibson [30] were used

to derive the necessary equations and to derive the necessary material properties.

Model Assumptions

To simplify the equations used in the study, a few assumptions and trade-offs had to be considered. First, model geometry was considered. The human hand model used for the study was assumed to be symmetric. Thus it was assumed that uniform radial heat generation occurred, and that within every symmetric radial coordinate ($r1 = r2$) the energy balance would equate to one-another. This reduced the equations of interest to a one-dimensional problem.

Second, we considered how to model the fabric itself. In order to use relevant literature, Gibson's [30] assumptions were followed - which assumed the fabric to be modeled as a hygroscopic porous media. Gibson modeled the fabric material as a joint system containing a solid phase, consisting of solid (e.g., polymer or cotton) fibers mixed with bound immobile water absorbed by the polymer matrix, a liquid phase consisting of free liquid water, and a gaseous phase consisting of water vapor plus inert air.

Lastly, we considered how to simultaneously combine the equations needed for heat and mass transfer for a two-fabric-layer control volume. Thus the model must account for heat transfer by conduction in all phases, convection in the gas and liquid phases, and latent heat release due to phase change from liquid to vapor phase. Radiation heat loss/gain is assumed to be negligible. For simplicity, the gas phase convection contributions due to external air movement (i.e. mars wind), are neglected. Moreover, it was assumed that all the sweat exiting the body had left in a gaseous phase. All excess buildup of sweat on the skin surface was assumed to drip off or wick into the fabric becoming immobile bound water. This condition simplified the problem by removing the need to account for free liquid water. We assumed free liquid water exists neither on the surface of the skin nor in the fabric layer.

Boundary and Initial Condition

The user begins at an equilibrium state. The skin surface is assumed to be 35C (308K), along with a constant perspiration rate of 9 $g^1m^{-3}h^{-1}$ (i.e. insensible perspiration) [28]. The steady state conditions were run and the following chart was produced in figure 3.12. We assume this temperature and humidity as T(t=0, x=i) condition. In the subsequent phase, the user is considered to be performing a physically-intensive activity, represented by a high heat flux and high sweat rate.

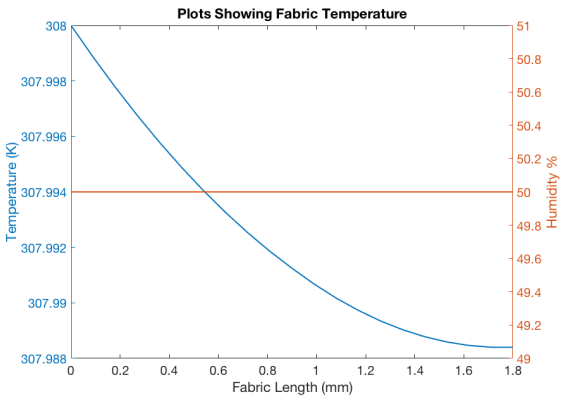

Figure 3.12: Initial condition of fabric using a steady state approximation following a 35C surface condition. 50% humidity and 20C cabin temperature were chosen for boundary.

Heat flux generated while being in an active state is assumed to be

$300 W m^{-2}$ whereas the sweat produced is assumed to be 240 $g^1 m^{-3} h^{-1}$ [28].

The cabin temperature resulting from the "open-loop" system is assumed to be warmed up to 20C with 50% humidity. These values were arbitrarily chosen as being comfortable for a person. Although the cabin pressure is pressurized by CO_2, the model will use dry air constants for ease of calculations.

Lastly, we assume the internal membrane to consist of two major components. A material that helps to absorb the water, and a material that helps conduct energy out of the system. The works of S.F. Neves [28], P. Chitrphiromsri [29] and Gibson [30] were used to derive the necessary material properties for such a blend of fabrics. Material properties are displayed on table 3.1.

Table 3.1: Properties of water, air, gas, and textile samples used for numerical simulation.** v is the water vapor property, a is the air property, w is the liquid water property and ds is the textile dry solid property

Observation	Parameter	Unit	Value	Source
Water, Air,	Cp_v	$Jkg^{-1}K^{-1}$	1862	[31]
& Water Vapor	Cp_w	$Jkg^{-1}K^{-1}$	4190	[31]
	Cp_a	$Jkg^{-1}K^{-1}$	1003	[31]
	ρ_w	$kgm{-}3$	1000	[31]
	k_w	$WK^{-1}m^{-1}$	0.60	[31]
	M_{H20}	$kgmol^{-1}$	$18.02{\times}10^{-3}$	[31]
	k_a	$WK^{-1}m^{-1}$	$2.56{\times}10^{-2}$	[31]
	M_a	$kgmol^{-1}$	$28.97{\times}10^{-3}$	[31]
	k_v	$WK^{-1}m^{-1}$	$2.46{\times}10^{-2}$	[31]
	R	$Jkg^{-1}K^{-1}$	8.314	[31]
	ϕ_{skin}	(-)	1.00	Chosen
	T_{skin}	(K)	308.15	Chosen
	v_{air}	ms^{-1}	0.5	Chosen
Membrane A Layer	k_{ds}	$WK^{-1}m^{-1}$	0.40	Chosen
Moisture Absorption	Cp_{ds}	$Jkg^{-1}K^{-1}$	1360	Chosen
	ρ_{ds}	$kgm{-}3$	250	[29]
	$Regain_{65\%}$	(-)	0.056	Chosen
	D_f/d_f	$m_{-1}s_{-1}$	4.5×10^{-5}	Chosen
	L	m	0.850×10^{-3}	Chosen
	ϵ_{ds}	(-)	0.269;	Chosen
	τ	(-)	2.49	[29]
Membrane B Layer	k_{ds}	$WK^{-1}m^{-1}$	0.48	Chosen
Temperature	Cp_{ds}	$Jkg^{-1}K^{-1}$	1285	Chosen
	ρ_{ds}	$kgm{-}3$	220	[29]
	$Regain_{65\%}$	(-)	0.041	Chosen
	D_f/d_f	$m_{-1}s_{-1}$	2.69×10^{-5}	Chosen
	L	m	0.95×10^{-3}	Chosen
	ϵ_{ds}	(-)	0.3;	Chosen
	τ	(-)	1.82	[29]

Transient Equations used for the model

The works of S.F. Neves [28], P. Chitrphiromsri [29] and Gibson [30] were used to derive the necessary equations for this section. For a full derivation, please refer to these literature or to appendix 5.2. The full written code, with comments is also provided.

Part 1: Energy Equation

$$\rho c_p \frac{\delta T}{\delta t} = \frac{\delta}{\delta x}\left(k_{eff}\frac{\delta T}{\delta x}\right) - \left(\Delta h_l + \Delta h_{vap}\right)\dot{m}_{sv} \tag{3.1}$$

The energy balance equation combines the effect of conductive losses and enthalpy changes occurring in a control volume. ρ is the effective density of the fabric which is calculated as a weighted average. C_p represents the weighted average of the effective specific heat in the fabric volume. T is the temperature measured kelvin while t is the time. The temperature changes will be calculated transiently for a 30 minute interval. Δh_l represents the enthalpy of transition from the bound water to free liquid water, Δh_{vap} is the enthalpy of evaporation per unit mass. The mass flux of vapor out of the fiber (or into the fiber if the value is negative) is represented by m_{sv}. The 1-D direction is measured by the x coordinate. k_{eff} is the effective thermal conductivity of the fabric which is a weighted average as well. The energy balance equation will be used to calculate the changes in temperature over the fabric length per time step.

Part 2: Solid phase continuity equation

$$\rho_w \frac{\delta}{\delta t}\left(\epsilon_{bw}\right) - \dot{m}_{sv} = 0 \tag{3.2}$$

As sweat slowly accumulates on the fiber and leaves the skin, the volume of bound water increases within the control volume increases. The solid phase continuity equation addresses these changes. ϵ_{bw} represents the volume fraction of bound water to the total volume of the control volume.

Part 3: Gas phase diffusivity equation

$$\frac{\delta}{\delta t}\left(\epsilon_\gamma \rho_v\right) = \frac{\delta}{\delta x}\left(D_{eff}\frac{\delta \rho_v}{\delta x}\right) + \dot{m}_{sv} \tag{3.3}$$

The gas phase diffusivity equations follow the changes in vapor density as a function of time and space. These equations were modeled off of Fick's laws of diffusion. D_{eff} represents the diffusivity of water vapor in air. ρ_v is the density of vapor for every node and ϵ_γ measures the total volume fraction of air and vapor in the control volume.

Part 4.1: Thermal Boundary Condition

$$\frac{\delta}{\delta x}\left(-k_{eff}\frac{\delta T}{\delta x}\right)\Big|_{x=0} = \left(q''_{convection}\right) - \left(\Delta h_l + \Delta h_{vap}\right)\dot{m}_{sv} \tag{3.4}$$

$$\frac{\delta}{\delta x}\left(-k_{eff}\frac{\delta T}{\delta x}\right)\Big|_{x=L_{Fab}} = -h_k\left(T_{air} - T_{x=L_{Fab}}\right) - \left(\Delta h_l + \Delta h_{vap}\right)\dot{m}_{sv} \tag{3.5}$$

Part 4.2: Mass Transfer Boundary Condition

$$\frac{\delta}{\delta x}\left(- D_{eff}\frac{\rho_v}{\delta x}\right)\Big|_{x=0} = \dot{m}_{sweat} + \dot{m}_{sv} \tag{3.6}$$

$$\frac{\delta}{\delta x}\left(- D_{eff}\frac{\rho_v}{\delta x}\right)\Big|_{x=L_{Fab}} = -h_m\left(\rho_{v,air} - \rho_{v,x=L_{Fab}}\right) + \dot{m}_{sv} \tag{3.7}$$

3.2.3 Results of numerically modeling heat and mass transfer for sweating during active use of EMU

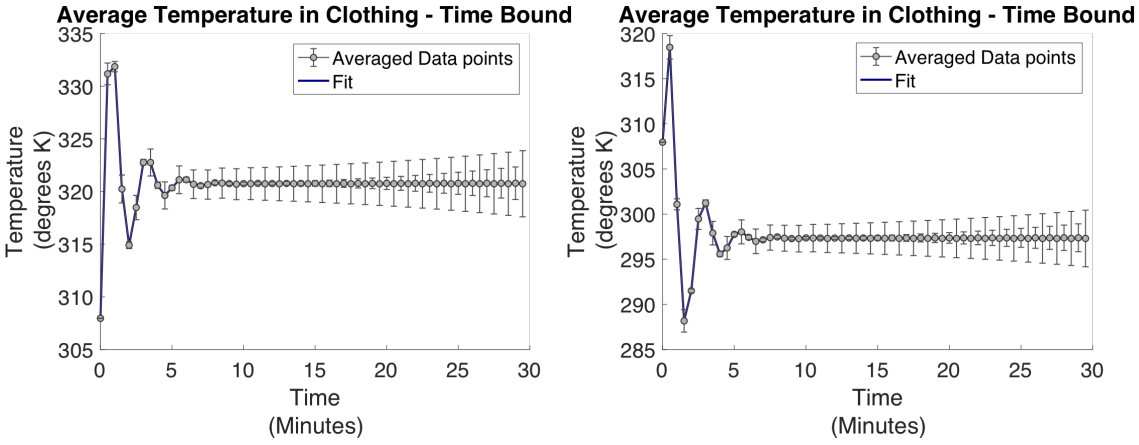

(a) EMU without LCG Effect **(b)** EMU with LCG Effect

Figure 3.13: The average temperature in the internal membrane of the suit with and without the effects of LCG

Figure 3.13 shows the effect on the average temperature of the fabric when a user is in an active state for 30 minutes. When the EMU is without the liquid-cooling garment the temperature is roughly 15 $^\circ K$ higher than the initial condition. From the graph, the average fabric temperature is closer to $322^\circ K$.

Liquid cooling garments are seen to have a significant impact on the temperature felt by the user. The LCG equipped device was seen to decrease temperature by roughly $15^\circ K$ and averaged to roughly $297^\circ K$.

Density of vapor along the fabric and the resulting temperature distribution also played a big role in the simulation. Figure 3.14 shows the effect of the suit with and without the LCG. Overall these results tend to show vapor density slowly increasing over time in the fabric. As sweat production slowly increases, so does the vapor density within the control volume. The density of vapor within the fabric when the LCG was present was roughly 0.47 kgm^{-3} whereas the density for the fabric without the the LCG was roughly 0.52 kgm^{-3}.

Adding a liquid phase to the model would have been beneficial, albeit adding much more complexity to the simulation. Although we see vapor density increasing in the non-LCG design, the simulation results don't necessarily explain how much more water remains within the fabric. The effect of how well the sweat was managed could be better understood. Furthermore, the higher temperatures felt in the non-LCG design could play a role in producing higher vapor density as well.

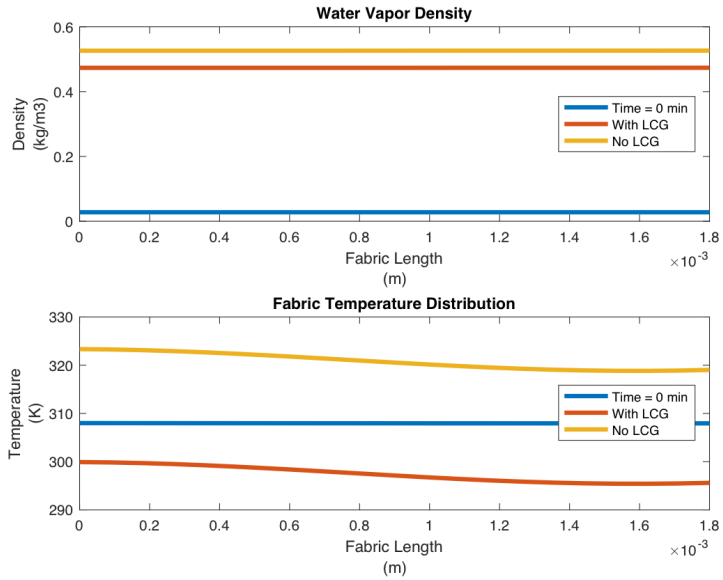

Figure 3.14:

Figure 3.15: Water Vapor and Fabric Temperature distribution after 30 minutes with/without LCG: *Blue t = 0min, Orange t = 30 min with LCG, Yellow t= 30 min without LCG*

Another important metric was how well the new open-loop system was able to remove heat. The requirement began as 263.763 W for matching pure convective/evaporative capacity of today's EMU and should equal or exceed the roughly 586.14 W thats currently removed from the LCG. From the results seen in figure 3.16 the LCG was seen to cool 461.5W using the LCG, while the non-LCG design was only capable of cooling 258.3 W.

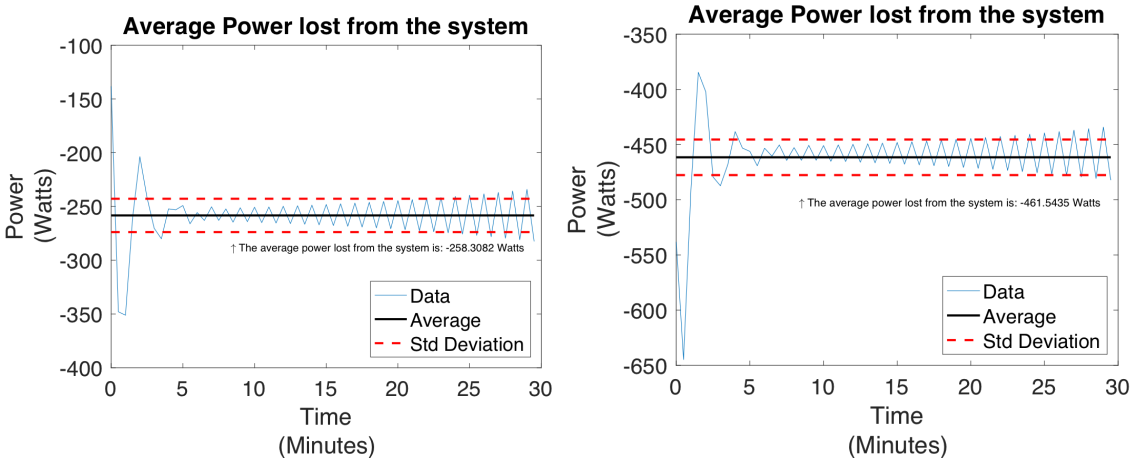

(a) EMU without LCG Effect **(b)** EMU with LCG Effect

Figure 3.16: Average work-rate of loss due to cooling mechanisms. *a) Convective & Evaporative; b) Convective, Evaporative & LCG*

These results fall well below the required cooling needs for the open-loop system. Convective and evaporative cooling will not be enough to cool the user

to a comfortable range. Furthermore, removing the LCG component from future suits will remain a priority. Thus the initial hypothesis of cooling will need to be changed for next generation Martian EMUs.

3.2.4 Discussion on numerical model results from the mars EMU model, and addressing areas of improvement

Based on the numerical simulation, we see that the "open loop" system is not capable of removing all the excess heat production during an active state without the use of a liquid cooling garment. The required heat loss is significantly lower than the value needed by a factor of two. We assume several factors play a role in this issue.

First, by restricting heat transfer to skin - inner membrane - ventilation layer, the cooling is limited to a very small region. Expanding this mechanism to involve the outer membrane and and the Martian ambient environment could be a better setup. In this scenario, forced convection in the ventilation layer, along with natural convection outside the suit could provide the necessary gradient for heat transfer without the need for a liquid cooling garment.

Another challenge with this particular numerical setup, is understanding the effect of ventilation. Specifically, it was rather difficult to predict how much water was truly trapped in the fabric. Since the equations used in this particular setup were restricted to gas diffusion in a porous solid, the liquid phase of water is ignored.

Two possible mechanisms of increasing the convective mass transfer can be introduced. Using the previous example of including the mars environment could be an excellent solution. The cold, dry CO_2 could would be a great sink for the excess moisture. Thus choosing a one-directional membrane for the outer layer, that doesn't allow any back-flow of Martian dust or foreign material could be beneficial.

Alternatively, using a desiccant to capture excess moisture near the outer membrane of the suit could be another method of promoting mass transfer. In such a mechanism the astronaut would switch suits when the desiccant is saturated, and simply keep switching suits throughout the day. This way the moisture is removed from the suit, and the captured water can be recycle for various purposes.

Lastly, this simulation used many assumptions to derive the temperature and change in density seen in the fabric. First and foremost, values and properties of air was used instead of dry, cold CO_2, since empirical values were hard to find. Second, heat flux and sweat were assumed to be constant at the skin surface. Thus, vasodilation, shivering or changes in metabolism were all ignored. Third, material properties also had to be reasoned out, rather than empirically tested. Since there was no empirical data on spacesuit materials, the team used material properties of common polyester, cotton and wool as estimates for the inner membrane. These assumptions add error into the model. Thus the numerical system that was used for the study does have its flaws, and requires more fine-tuning for future testing. However, we feel the model developed was a strong first step.

3.2.5 Future steps for heat transfer mechanism

Overall the team recommends a few next steps based on the findings of this report.

1. Use of Thermal Manikin

Thermal manikin are robot models that can represent human skin conditions for the testing of thermal environments [32]. These models mimic human behavior by heating up their core or shell to represent skin temperature, and can even mimic perspiration. The use of thermal human manikins could provide a significant upgrade over numerical models as several material properties could be tested repeatedly, for a more realistic understanding of the properties and limitations of the fabric. These tests could provide empirical results which will represent a more realistic take on the effects of the suit. Thus a great next step would be to use the numerical model provided to test a few critical proprietaries (i.e mass diffusivity, specific heat, or thermal conductivity of the fabric) and then collect empirical data on the true behavior of the fabric.

2. Improved Heat & Mass transfer model

The numerical model that was developed for this study was limited to the interactions between the skin and the open-loop ventilation component. However, if one could include the entire thermal boundary (ie. body core to the mars environment) by rewriting Dr.Kuznetz's 41-Node man, that would provide key insights to the effects of heat transfer. Furthermore by expanding the equations to include the liquid phase of water, the user will be able to predict how much sweat was removed and quantify the effectiveness of the ventilation system.

3. Understanding the effects of cold dry CO_2 for mass convection

One key insight that we hadn't quite understood was the Martian environment itself. The parameters that we would want to understand better include, how well sweat can be absorbed by the Martian environment, quantifying various transport properties for refining the numerical model, and understanding how well the mars environment would work as a heat sink. Therefore lab testing of CO_2 in a vacuum environment could provide insight to the feasibility of the open loop system, and its effectiveness for heat and mass transfer.

Robotic augmented system for gripping assistance

3.3.1 Overall architecture

The whole robotic assistive system is combined of the sensor and the actuation part. Pressure sensors attached to the glove fingertip recorded force during gripping motion. The first filter is applied to eliminate noise and to prevent saturation. The second filter (PID control) is then applied to generate desired force. Detailed procedure can be seen in the Appendix.

3.3.2 Sensors

As a space glove, our product has to be able to sense the environment, including ambient temperature, pressure and humidity, so that it can alert the user promptly if something is wrong. Besides, in order to enhance the force of the user's hand, the robotic assistive system needs to detect the motion of the hand first. Therefore, the sensor integration is a critical part of this glove.

For the prototypes, the sensors will be connected to the Arduino board as shown figure 3.17. We will have several fingers connected to actuators and sensors, including but not limited to the thumb, index finger and the middle finger, which should be sufficient to help the gripping force.

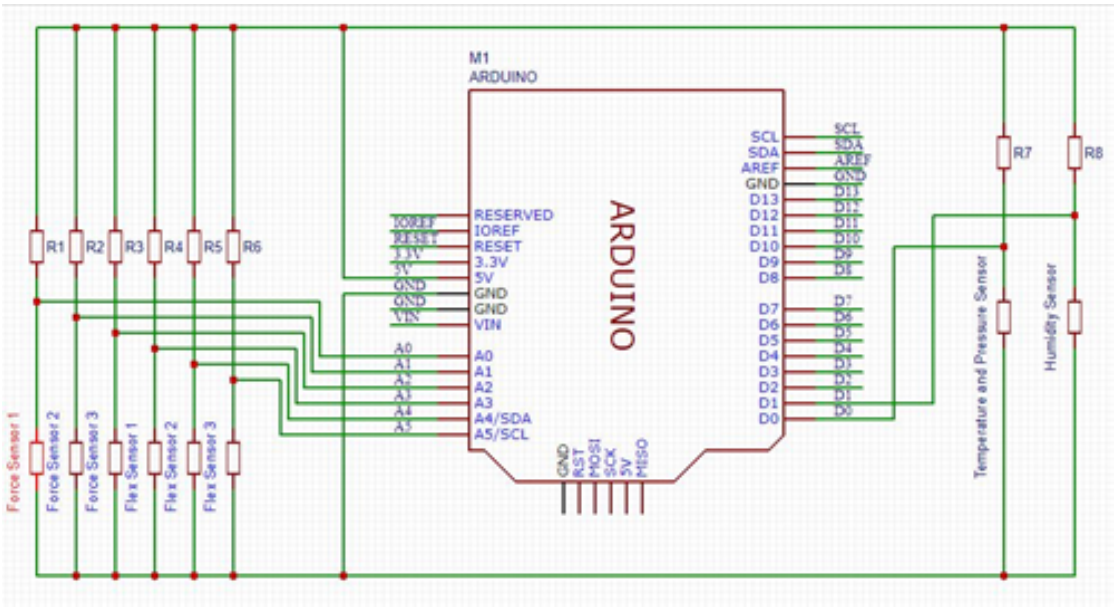

Figure 3.17: Arduino Schematic

To fully capture the motion and the environment of the hand, three types of sensors are used: force sensors, flex sensors and temperature and pressure sensors as shown in figure 3.18.

The force sensors are placed at the fingertips inside the glove and they can sense the pressure applied on them. As shown in figure 3.19, the pressure signals are processed by an algorithm to be converted to force, and then plotted against time. For the purpose of demonstration, only two force sensors, distinguished by

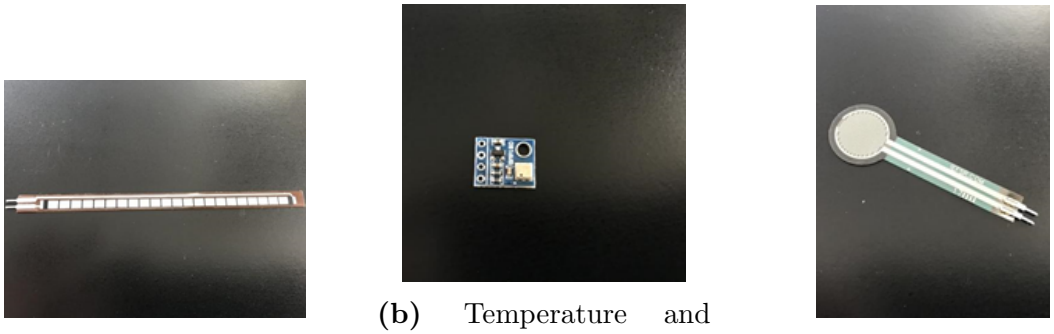

(a) Flex Sensor

(b) Temperature and Pressure Sensor

(c) Force Sensor

Figure 3.18: Selection of Sensors

different colors, are being used to get the results in this picture. The processed force signals are ready to be used as the inputs of the control algorithm of the robotic assist system.

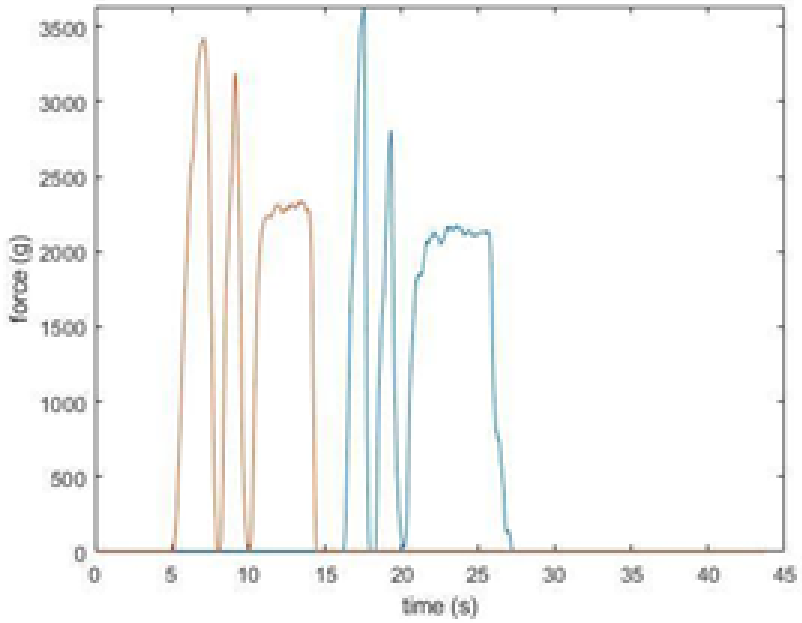

Figure 3.19: Force Sensor Readings (Finger 1: Orange, Finger 2: Blue)

The flex sensor detects the bending angle of itself, therefore, they will be placed on the outside of the glove along each finger to measure the position of the fingers. This will also be one of the inputs for the robotic assist algorithm. Figure 3.20 is a demonstration of what the signals will look like. Again, only two flex sensors are used here.

The temperature and pressure sensor can sense temperature and pressure at same time. It will be placed at the back of the hand outside of the glove to detect the ambient environment without affect the mobility of the hands. Figure 3.21 is the sample output of the sensor. This signal will be used to monitor the surroundings of the hand.

As mentioned before, humidity is also an important factor of the environment that needed to be measured. Therefore, a humidity sensor would be placed at the center of the back of the hand along with the temperature and pressure sensor. A

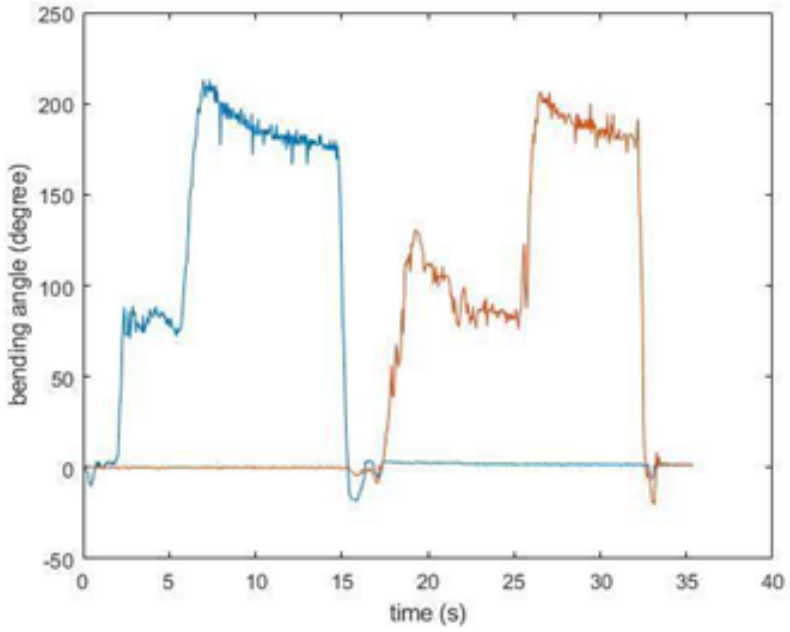

Figure 3.20: Flex Sensor Readings (Finger 1: Orange, Finger 2: Blue)

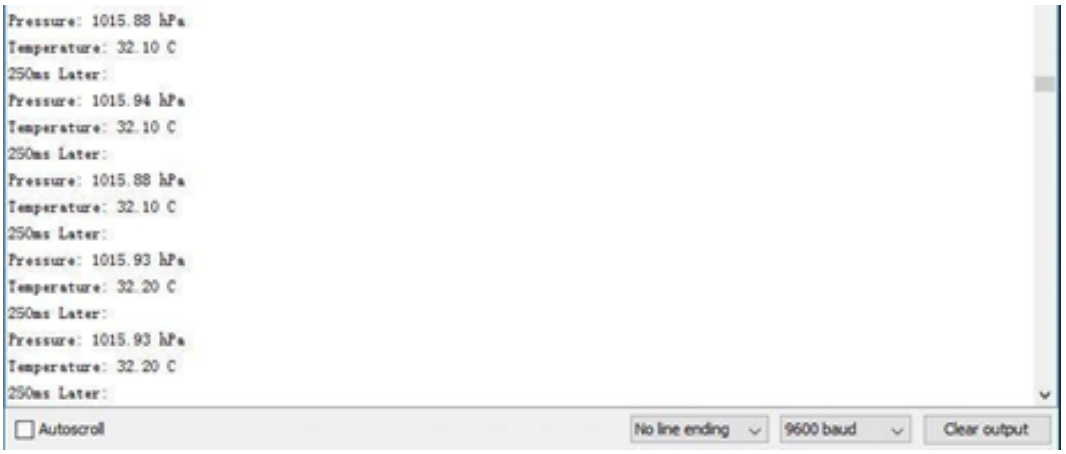

Figure 3.21: Temperature and Pressure Sensor Output Readings

sample output is shown in figure 3.22.

All the sensors and actuators will be combined together to make the prototypes. The purpose of the prototypes is to validate and refine the tendon design and make sure that it can indeed provide an assistive force to grasping task and further details will be discussed in the section below.

■ 3.3.3 Servo actuator and Linear actuator

The actuating and controls components run parallel to the sensing component. Using the sensing inputs, the actuation component assists user hand motions. Two potential candidates to assist user hand motions have been identified and tested: servo motors and linear actuators. Servo motors are low in weight, cost, and are easy to implement, test, but are limited in their force generating capacity. Linear actuators, on the other hand, are more expensive and complex, but provide enhanced force generating capacity.

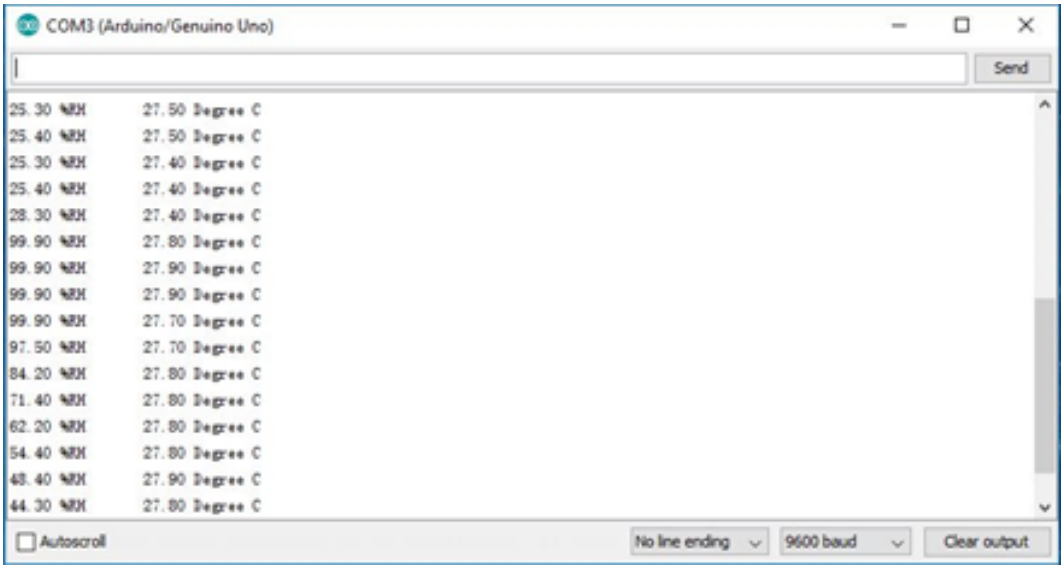

Figure 3.22: Relative Humidity and Temperature Readings

We designed, manufactured, and tested two prototypes based on our identification of candidate actuating and controls components.

■ 3.3.4 Prototype 1 (with SG90 micro servo motor)

The first prototype (figure 3.23.A) consists of an ordinary glove, several paper rings placed around the index finger of the glove, a string that is mounted onto the rings and a SG90 micro servo motor that pulls the string at the bottom. The SG90 micro servo (figure 3.23.B) is a light-weight (9 grams) servo motor that provides up to 1.8 N.cm of torque. We successfully implemented this prototype that demonstrated the glove's ability to assist gripping. With the pressure on the fingertip part of the glove while gripping, pressure sensor takes in the signal and control algorithm process it to the actuator part. As the gripping movement continues, the tendon pulls in a direction parallel to that of the finger. Thus enables users to accomplish their task with lower gripping force.

This prototype demonstrated the feasibility of the concept and helped us identify areas requiring revision. First, the biggest disadvantage of servo motor is the insufficient torque it provides. Based on our research and other similar products, an additional 40 N of force is required to make a significant difference in gripping assist. However, the stall torque of SG90 micro servo is only 1.8 N•cm, which is insufficient per the required force generation specifications.

Further, the first prototype helped us identify challenges with respect to material selection. We observed that the tendon was slipping left and right when it should have been purely longitudinal, causing unwanted shear force and thus wasting the impact of the torque. Thus, we decided that either the geometric design should preclude shear loading or the material itself should accommodate a substantial shear force without deformation or failure.

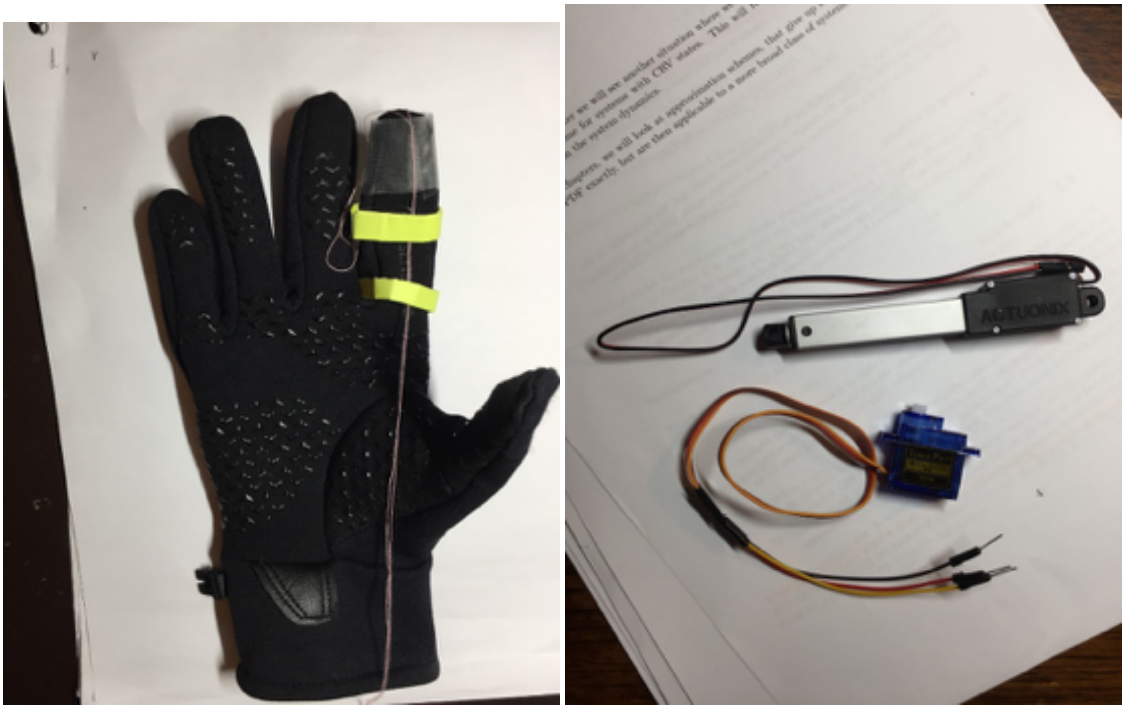

(a) Servo Motor Prototype **(b)** Linear and Servo Actuator

Figure 3.23: Actuation-Sensor Prototype

3.3.5 Prototype 2 (with L12 Micro Linear Actuator)

To solve challenges mentioned above, several design changes were made to improve the performance of the second prototype. First, servo motors were replaced with L12 Micro Linear Actuators (figure 3.24.B). We replaced the paper rings with 3-D printed plastic rings to make it more robust. In addition, we applied this design to the thumb of this glove so that we have two fingers equipped with gripping assist. To guide the tendons of these two fingers, we added a joint at the bottom of the glove that is also 3-D printed. We also switched the material of the tendon from sewing threads to polyester braid rope. Lastly, sensing and control algorithm is also modified to accommodate to the linear actuators.

We used a hand dynamometer to measure the gripping force produced by these two fingers and the results showed that it will be able to provide 13 N of force. Tendon rings and tendon channel also helped directing tendons in a way that they can mitigate undesired shear force. Sensing and control algorithms also improved the comfort of this prototype throughout the operation. Still, improvement on several parts can be done. For the actuator part, L12 linear actuator with longer stroke length can be applied to extend pulling range. Also, it would be better to customize tendon rings and channel to fit individual hand. Lastly, more suitable tendon material and channel design is still under research.

3.3.6 Ongoing and Future Work

Based on previous prototypes, future prototypes will be fixed with the L12 Micro Linear Actuator. The third prototype should be designed with L12 50mm

(a) Prototype 2 **(b)** Tendons Ring and Tendons

Figure 3.24: Linear-Actuator Prototype

Micro Linear Actuator and modified tendon rings and channel. Focus of this prototype would be to design customized tendon rings and channel that further smoothen the operation. Channel design will further focus on minimizing friction generated. Also, an user alert system should be developed in the future iterations of prototype to indicate the environment within the glove.

Part 4

Recommendations

For those interested in working on this project, Team Vanguard has laid a foundation to further develop this concept. With further funding and manpower, this product could be redesigned to increase performance, minimize size, and improve controls.

Future work may involve the development of a more sophisticated and robust heat transfer model to understand the thermal mechanism better and to choose the proper material for different layers of the glove. As previously mentioned, the robotic assist system also needs to be improved in terms of motor selection, tendon material selection and tendon channel design. And it is critical to test out the ideas and solutions with minimum viable prototypes along the way.

To anyone working on this project in the future, Team Vanguard is willing to provide any information related to this project upon request. We are happy to be part of the transformation towards Mars colonization.

References

[1] Dashevsky, E. "SPACE for SALE: How the Private Space Industry Will Reinvent Economics, Exploration, and Humanity." PC Magazine, Aug. 2017, p. 77.

[2] "The Space Tech Market Map: 57 Startups Charting The Final Frontier." CB Insights Research Aug. 2017, www.cbinsights.com/research/space-tech-startups-market-map/ .

[3] "Space Tech Funding Drops Back To Earth While Deals Push Up." CB Insights Research, 21 July 2017, www.cbinsights.com/research/space-tech-startup-funding/.

[4] Wall, Mike. "Elon Musk Publishes Plans for Colonizing Mars." Scientific American, 16 June 2017, www.scientificamerican.com/article/elon-musk-publishes-plans-for-colonizing-mars/.

[5] Cofield, C. "Lockheed Martin Reveals Plans for Sending Humans to Mars." Scientific American, 29 Sept. 2017, www.scientificamerican.com/article/lockheed-martin-reveals-plans-for-sending-humans- to-mars/.

[6] Vartan S., "STYLIN' ON MARS", *Newsweek Global*, vol. 169, no. 3, pp. 48-51, 2017.

[7] Gernhardt, M. L., Abercromby, A. J., Bekdash, O. S., Norcross, J. R., House, N., Jones, J. A., & Tuxhorn, J. A. (2017). Evidence Report: Risk of Injury and Compromised Performance due to EVA Operations.

[8] Thomas K.S., McMann H.J. (2012) *The basics of spacesuits*. In: U. S. Spacesuits. Springer Praxis Books. Springer, New York, NY

[9] ElKoura, George, and Karan Singh (2003). "Handrix: animating the human hand." Proceedings of the 2003 ACM SIGGRAPH/Eurographics symposium on Computer animation. Eurographics Association.

[10] Appendino, S., Battezzato, A., Chen Chen, F., Favetto, A., Mousavi, M. and Pescarmona, F. (2014). "Effects of EVA spacesuit glove on grasping and pinching tasks", *Acta Astronautica*, vol. 96, pp. 151-158.

[11] Nier, A. and McElroy, M. (1977). Composition and structure of Mars' Upper atmosphere: Results from the neutral mass spectrometers on Viking 1 and 2. *Journal of Geophysical Research, 82(28)*, pp.4341-4349.

[12] Strauss, S., Krog, R. L., and Feiveson, A. H. (2005). Extravehicular mobility unit training and astronaut injuries.*Aviation, space, and environmental medicine*, 76(5),pp. 469-474.

[13] Jordan, N. C., Saleh, J. H., and Newman, D. J. (2006). The extravehicular mobility unit: A review of environment, requirements, and design changes in the US spacesuit. *Acta Astronautica*, 59(12), pp.1135-1145.

[14] Frazer, A. L., Pitts, B. M., Hoffman, J. A., and Newman, D. J. (2002). Astronaut Performance: Implications for Future Space Suit Design. *IAF abstracts, 34th COSPAR Scientific Assembly.*

[15] Parker Jr, J. F., and West, V. R. (1973). Bioastronautics Data Book: NASA SP-3006.*NASA Special Publication, 3006.*

[16] Annis, J. F., and Webb, P. (1971). *Development of a space activity suit.*

[17] Abts, K. J. (1999). U.S. Patent No. 6,000,059. Washington. *DC: U.S. Patent and Trademark Office.*

[18] Jordan, N. C., Saleh, J. H., and Newman, D. J. (2006). The extravehicular mobility unit: A review of environment, requirements, and design changes in the US spacesuit. *Acta Astronautica*, 59(12), pp.1135-1145.

[19] Abts, K. J. (1999). U.S. Patent No. 6,006,355. Washington.*DC: U.S. Patent and Trademark Office.*

[20] Shepard, L., Durney, G., Case, M., Pulling, R., Rinehart, D., Bessette, R., ... Wise, R. (1973). U.S. Patent No. 3,751,727. Washington.*DC: U.S. Patent and Trademark Office.*

[21] Ross, A., Rhodes, R., Graziosi, D., Jones, B., Lee, R., Haque, B. Z. G., and Gillespie, J. W. (2014, July). Z-2 Prototype Space Suit Development. *44th International Conference on Environmental Systems.*

[22] Y. Pang, X. Liu and X. Guanghui, "Extravehicular Space Suit Bearing Technology Development Research", *IOP Conference Series: Materials Science and Engineering* , vol. 187, p. 012014, 2017.

[23] Marcy, J. L., Shalanski, A. C., Yarmuch, M. A. R., and Patchett, B. M. (2004). Material choices for mars. *Journal of materials engineering and performance*, 13(2), pp.208-217.

[24] Lubach, D. and Beckers, P. (1992). Wet working conditions increase brittleness of nails, but do not cause it. *Dermatology*, 185(2), pp.120-122.

[25] Anon, (2018). [online] Available at: https://www.nasa.gov/audience/ foreducators/spacesuits/home/clickablesuitnf. [Accessed 26 Apr. 2018]

[26] Kuznetz, L. (1979). A two-dimensional transient mathematical model of human thermoregulation. *American Journal of Physiology-Regulatory, Integrative and Comparative Physiology*, 237(5), pp.R266-R277.

[27] Midwest Research Institute (Kansas City, M. (1975). *Liquid cooled garments*. [online] Core.ac.uk. Available at: https://ntrs.nasa.gov/archive/nasa/casi.ntrs.nasa.gov/19750007244.pdf [Accessed 27 Apr. 2018].

[28] Neves, S.F., Campos, J. and Mayor, T. (2017). Effects of clothing and fibres properties on the heat and mass transport, for different body heat/sweat releases. *Applied Thermal Engineering*, 117, pp.109-121.

[29] Chitrphiromsri, P. and Kuznetsov, A. (2003). Modeling heat and moisture transport in firefighter protective clothing during flash fire exposure. *Heat and Mass Transfer* 1(1), pp.206–215.

[30] Gibson PW (1996) Multiphase heat and mass transfer through hygroscopic porous media with applications to clothing materials. *Technical report Natick/TR-97/005*. U.S. Army Natick Research, Development, and Engineering Center, Natick, Massachusetts

[31] M.W. Haynes, D.R. Lide, *Handbook of Chemistry and Physics*, (n.d.) 6-15-20. [online] Available at:http://www.hbcpnetbase.com/ [Accessed 29 Apr. 2018].

[32] Holmér, Ingvar. Thermal manikin history and applications, *European Journal of Applied Physiology*, vol. 92, no. 6, pp. 614-618, 2004.

Part 5

Appendix

1. Derivation of Heat & Mass Transfer Equations
2. Transient Solution for Sweating Mechanism on Fiber Volume

■ Derivation of Heat & Mass Transfer Equations

Thomas Chengattu

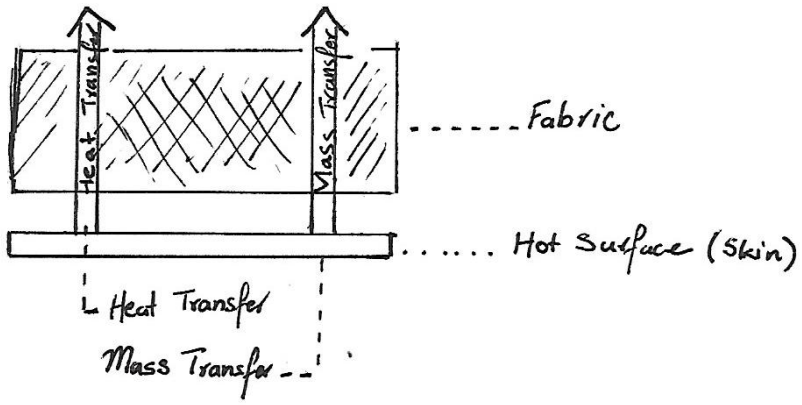

The Following notes are used to create a detailed transfer model to analyse the effect of fabric material characteristics (outer - surface emissivity, tortuosity, and fraction of fiber) and fiber properties (affinity with water, diffusion coeffeint, thermal conductivity, density, specific heat)

Part 1: Mass Transfer of Sweat Through Fabric

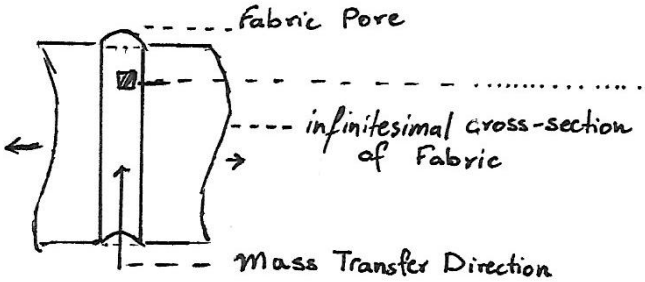

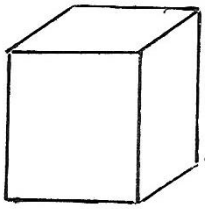

Control Volume

Volume of dry solid Fiber
Volume of bound water
+ Volume of occupied gas
Total Volume

$$V_{ds} + V_{bw} + V_g = V_{Tot}$$

$V_g = V_a + V_{W\_V}$ } gas includes air and water vapor.

Volume Fraction ... * $\epsilon_{ds} + \epsilon_{bw} + \epsilon_g = 1$

Assumptions Employed: (What we choose to ignore*)

i. Gas phase convection contributions due to external air
   → i.e wind felt outside on mars
   → Chosen for simplicity

ii. Sweat produced by the body is considered in vapor state
   → Chosen For simplicity

iii. Moreover any extra liquid sweat which might normally build up on the surface of skin will drip off or wick into the fabric fibers contributing to bound water.
   →* Free liquid water neither exists on the surface of the skin nor in the the fabric layer.

Thomas Chengattu

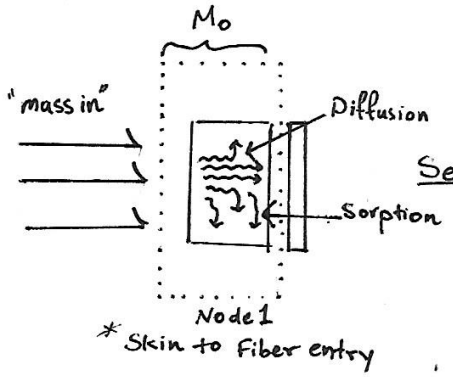

One-Dimensional Problem Formulation

Section 1: Understanding the input condition

- m_s → Mass introduced through sweat production ($kg/m^2 \cdot s$)
- m_{dif} → Mass diffused into the fiber (. . .)
- m_{sv} → Mass of vapor involved in "sorption" (. . .)

* We will consider a medium for which stationary medium approximation holds — Mass transfer approximated as occuring only via diffusion & sorption and ~~negligible~~ negligible advection.

- Assuming water behaves like an ideal gas, we creat the following "time-mass" equation

$$\begin{cases} \dot{M}_o = \dot{m}_s - \dot{m}_{diff} - \dot{m}_{sv} \ldots . \left(kg/m^2 \cdot s \right) \\ \dfrac{dM_o}{dt} = \dot{m}_s - D_{eff}\left(\dfrac{P_o - P_i}{\Delta x}\right)\left(\dfrac{M_{H_2O}}{R\,T_o}\right) - m_{sv} \end{cases}$$

Variables used

- P_o - vapor pressure at Node "i"
- P_i - vapor pressure at Node i+1
- Δx - thickness of section
- M_{H_2O} - Molar Mass of water
- R - Gas Constant
- T - Temperature at "T_i"

* We assume that change in vapor pressure will be caused due to the change in vapor density for water vapor.

Mass ~~Diffusion~~ Diffusion Equation:

For Node 1:

$$\frac{\partial(\epsilon_g \cdot \rho_v)}{\partial t} = \dot{m}_{s*} - D_{eff} \cdot \nabla^2 \rho_v - \dot{m}_{sv}$$

Thermodynamic Relations

- partial pressure consideration

Total Gaseous Pressure = Air Pressure + Water Vapor Pressure

$$P_g = P_a + P_v \quad : P_g = \text{constant}$$

$$P_v = \rho_v \left(\frac{R}{M_{H_2O}}\right) T \quad : \rho_v \rightarrow \text{calculated using diffusion}$$

$$P_a = \rho_a \left(\frac{R}{M_{air}}\right) T \quad : P_a = P_g - P_v$$

* $P_v(t=0) = 0$; $P_g = P_a(t=0)$: Dry Condition

Thomas Chengattu

Solid Phase Continuity Equation for Node 1

Density of water → $\rho_w \frac{\partial(\epsilon_{bw})}{\partial t} = -\dot{m}_{sv}$

Bound Water: Refers to water molecules that become immobile and attached onto the fabric. The volume fraction ϵ_{bw} will slowly increase as a function of time due to sorption.

$$*\epsilon_{bw}(t=0) = 0$$
$$\epsilon_g + \epsilon_{ds} = 1 \quad (@t=0)$$
$$\rho_{gas} = \epsilon_g(\rho_v + \rho_a)$$

} Volume fraction considerations. ϵ_{bw} : volume fraction of Bound Water

Mass Flux of Vapor Out of Fiber

$$\dot{m}_{sv} = \frac{D_{solid}\,\rho_{ds}}{d_f^2}\,(R_{f,total} - R_{f,skin})$$

Material property ……→
- D_{solid} → Diffusivity of Bound Water in the solid phase
- ρ_{ds} → Density of dry solid
- d_f → Average Fiber diameter

Moisture Regain is defined as the weight of water in a textile fabric expressed as a percentage of the oven dry weight of the textile

$$R_{f,total} = \frac{\epsilon_{bw}\rho_{bw}}{\epsilon_{ds}\rho_{ds}}$$

R_{fskin} can be calculated using the equilibrium volume fraction of bound water $\epsilon_{bw,eq}$. This is obtained from the sorption relationship.

$$\epsilon_{bw,eq} = 0.578 \cdot R_{f,\phi=65} \cdot \left(\epsilon_{ds}\frac{\rho_{ds}}{\rho_{bw}}\right) \cdot \phi \cdot \left[\frac{1}{(0.521+\phi)} - \frac{1}{(1.262-\phi)}\right]$$

- $R_{f,\phi=65}$ → Fabric Regain at 65% relative humidity
- ϕ : Relative humidity, defined as follows.

$\phi = P_v / P_{sat}$: The relative vapor pressure of water related to the saturation vapor pressure

- $P_{sat} = 614.3 \cdot \exp\left\{17.06\left[\frac{(T-278.15)}{(T-40.25)}\right]\right\}$

- $R_{fskin} = \frac{\epsilon_{bw,eq}(T, P_v)\cdot\rho_{bw}}{\epsilon_{ds}\cdot\rho_{ds}}$ ←…… $\epsilon_{bw,eq}$ is therefore related by the the partial pressure of water vapor, and the temperature at its position

Thomas Chengatha

Calculating Mass Transfer leaving the system.

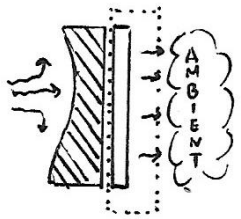

- Assume mass transfer convection, transporting excess fluid out of the system.

$$\dot{M}_{end} = \dot{m}_{diff} - \dot{m}_{convection}$$

$$\frac{\partial(\epsilon_g \rho_v)}{\partial t} = D_{eff} \nabla^2 \rho_v - h_m (\rho_{v,air} - \rho_v)$$

"$kg/m^3 \cdot s$" leaving the system

*we will keep track of how much mass escapes the system. This will be equal to $\dot{m}_{convection}$ ($\pi/4 \, d_f^2$)

$$\dot{k_g} = \dot{m}_{convection} \left((x_{end} - x_o) \cdot \left(\frac{\pi}{4} d_f^2 \right) \right)$$

$$h_m = \frac{h}{\rho_a \cdot C_{p\_a} \cdot Le^{2/3}} \quad ; \; Le = \frac{Sc}{Pr} = \frac{\alpha}{D_{AB}}$$

- Lewis Number relates mass and thermal diffusivity

Thomas Chengattu

Part 2 : Heat Transfer through fabric

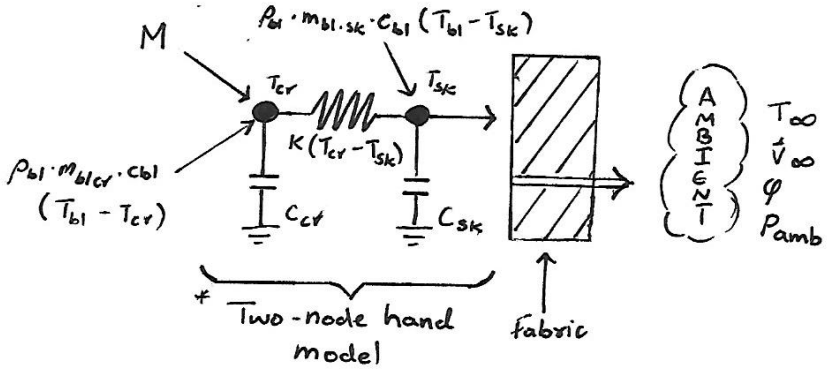

Energy Equation for Fabric

We will have two situations. One will handle a constant heat flux and respective sweat production. The other will involve the 2-hand model as described in "K. Katić et al."

The following derivation will ~~boil~~ boils into a constant $\dot{q}_{gen}$ term during rest and excersise phase based on "S.F Neves et al."

Node 1 :

$$\rho c_p \frac{\partial T}{\partial t} = -k_{eff} \nabla^2 T - (\Delta h_l + \Delta h_{vap}) \dot{m} + \dot{q}_{gen}$$

a) ρ: effective density of the Fabric (averaged)

$$\rho = \varepsilon_{bw} \rho_{bw} + \varepsilon_{ds} \rho_{ds} + \varepsilon_g (\rho_v + \rho_{air})$$

b) C_p : specific heat of the fabric (averaged)

$$C_p = \frac{\varepsilon_{bw} \rho_{bw} (c_p)_w + \varepsilon_{ds} \rho_{ds} (c_p)_{ds} + \varepsilon_g [\rho_v (c_p)_v + \rho_a (c_p)_a]}{\rho}$$

c) k_{eff} : effective Thermal Conductivity of the Fabric

d) Δh_l : enthalpy transition from bound water to free liquid water

$$\Delta h_l = 1.95 \times 10^5 (1 - \varphi) \times \left[\frac{1}{(0.2 + \varphi)} + \frac{1}{(1.05 - \varphi)} \right]$$

Thomas Chengottu

e) Δh vap : # enthalpy of vaporization per unit mass

$$\Delta h_{vap} = 2.792 \times 10^6 - 160T - 3.43T^2$$

f) $\dot{m} = \dot{\rho}_v \cdot dx \cdot dy \cdot dz$

$= \dot{\rho}_v \cdot (x_{i+1} - x_i)\left(\frac{\pi}{4} df^2\right)$ } mass flow rate of water vapor determined by mass transfer

g) $\dot{q}_{gen}$ = constant

- Based on literature from "S.F. News"
  - excersise phase → 300 W-m^{-2}
  - Rest phase → 65 W-m^{-2}

Boundary Nodes

Fabric emissivity

5.67×10^{-8} W/m^2.K^4

$$\rho C_p \frac{\partial T}{\partial t} = \underbrace{k_{eff} \nabla^2 T}_{\text{Heat Diffused into Boundary}} - \underbrace{h_c^{conv} \left(T_{amb} - T_i\right)_{x=L}}_{\text{Heat lost due to convection}} - \underbrace{\varepsilon_r \sigma \left(T_{amb}^4 - T_i^4\right)_{x=L}}_{\text{Heat loss due to radiation}}$$

The convective heat transfer coefficient was calculated with the assumption that the hand ~~is~~ area is covered by clothing

* Assuming $Re \cdot Pr > 0.2$

$$Nu = \frac{h_c^{conv} \cdot d_{hand}}{k_a}$$

d_{hand} → diameter of hand

k_a → conductivity of air

$$= 0.3 + \frac{0.62 \cdot Re^{1/2} \cdot P_r^{1/3}}{\left[1 + (0.4/P_r)\right]^{1/4}} \cdot \left[1 + \left(\frac{Re}{282{,}000}\right)^{5/8}\right]^{4/5}$$

* $h_c^{conv} = \frac{Nu \cdot k_a}{d_{hand}}$

Thanas Chengattu

Part 3: System Inputs & Boundary Conditions

Section 1: Fabric Properties (optional → multilayer fabrics)

k_{ds}	Thermal Conductivity of Dry Fiber	$\left(\frac{W}{K \cdot m}\right)$
C_{p_ds}	Specific heat of Dry Fiber	$\left(\frac{J}{kg \cdot k}\right)$
ρ_{ds}	Density of dry Fiber	$\left(kg/m^3\right)$
$Regain_{f(\phi=65)}$ ..	Regain at a humidity of 65%	$(-)$
D_{solid} ...	Diffusioity of water in fiber	$\left(\frac{1}{s}\right)$
d_f	Average Fiber Drameter	(m)
L	overall thickness of material	(m)
ε_{ds}	Volume fraction of Dry Solid	$(-)$
τ	Fabric Tortuosity	$(-)$
T_o	Fabric Initial Temperature	(^oK)
φ_o	Initial Humidity	$(-)$

(optional - Multilayer fabric)

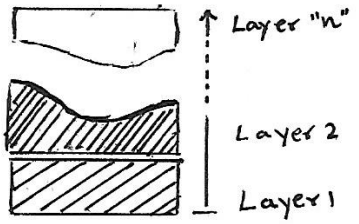

Section 2: Water, Air, Gas Properties

C_{p_v}	Specific heat - vapor	$\left(\frac{J}{kg\,k}\right)$
C_{p_w}	Specific heat - water	$\left(\frac{J}{kg\,k}\right)$
C_{p_a}	Specific heat - air	$\left(\frac{J}{kg\,k}\right)$
ρ_{bw}	density of bound water	$\left(kg/m^3\right)$
k_w	Thermal conductivity of water	$\left(\frac{W}{K\,m}\right)$
M_{H_2O}	Molar mass of water	$\left(kg/mol\right)$
M_a	Molar mass of air	$\left(kg/mol\right)$
k_v	Thermal conductivity of vapor	$\left(\frac{J}{kg\,k}\right)$
k_a	Thermal conductivity of air	$\left(\frac{J}{kg\,k}\right)$

Thomas Chengattu

Part 3: Numerical Simulation of Heat & Mass Transfer through clothing.

Each timestep, we update the density of the water vapor. Then we update the volume fraction of the bound water. Then we calculate the mass flow from the above equations to relate the enthalpy involved in evaporation and bound to liquid water energy losses – which will help to solve the temperature. Lastly we solve for the new relative humidity at the next time step using the ~~pressure~~ vapor pressure and temperature.

→ We will solve using second-order discretization scheme, a time-step of 0.01s, and the Crank Nicolson technique.

Section 1: Node 1

Pre-Amble

$$\varphi_0 \cdot P_{sat}(T_0) = P_{v0,x=0,t=0} \qquad \epsilon_{g,x=0,t=0} = 1 - \epsilon_{ds} - \epsilon_{bw,x=0,t=0}$$

$$P_g - P_{v0,x=0,t=0} = P_{a,x=0,t=0}$$

Order of Solving:

mass Transfer

① $$\epsilon_{g,x=0,t=0}\left(\frac{\rho_i^{t+1} - \rho_i^{t}}{\Delta t}\right) = \dot{m}_s - D_{eff}\left(\frac{P_{i+1}^{t} - P_i}{\Delta x^2}\right) - \dot{m}_{sv}(\epsilon_{bw0}, \varphi)$$

$\dot{m}_s$ ↓ $(kg/m^3\text{-}s)$

② $$\rho_w\left(\frac{\epsilon_{bw,i}^{t+1} - \epsilon_{bw,i}^{t}}{\Delta t}\right) = \frac{D_{solid} \cdot \rho_{ds}}{df^2} \cdot \left(\epsilon_{bw,i}^{t} \cdot \frac{\rho_{bw}}{\epsilon_{ds}\rho_{ds}} - R_{f,skin}(\varphi)\right)$$

heat Transfer

③ $$\rho C_p\left(\frac{T_i^{t+1} - T_i^{t}}{\Delta t}\right) = -k_{eff}\left(\frac{T_{i+1}^{t} - T_i^{t}}{\Delta x^2}\right) - (\Delta h_{vap}(\varphi) + \Delta h_{vap}(T))\dot{m}$$

$$(\dots) + \dot{q}$$

$$P_{v1,x=0,t=1} = \rho_{v1,x=0,t=1} \cdot \frac{R}{M_v} T_i^{t+1}$$

Reset humidity at $t=1\dots$

$$*\varphi_{0,x=0,t=1} = \frac{P_{v,t=1,x=0}}{P_{sat}(T_0^{t=1})}$$

Thomas Chengalath

Section 2: Node [i+1, n-1]
(Interior Nodes)

Preamble

- $\varphi_n \cdot P_{sat}(T_n) = P_{vn, x=n\Delta x, t=0}$
- $P_g - P_{vo, x=n\Delta x, t=0} = P_{a, x=n\Delta x, t=0}$
- $\epsilon_{g, x=n\Delta x, t=0} = 1 - \epsilon_{ds} - \epsilon_{bw, x=n\Delta x}$

① $\epsilon_{g, x=n\Delta x, t=0}\left(\frac{\rho_n^{t+1} - \rho_n^t}{\Delta t}\right) = D_{eff}\left(\frac{P_{n+1}^t - 2P_n^t + P_{n-1}^t}{\Delta x^2}\right) - \dot{m}_{sv}(\epsilon_{bw0}, \varphi)$

② $\rho_w\left(\frac{\epsilon_{bw,n}^{t+1} - \epsilon_{bw,n}^t}{\Delta t}\right) = \frac{D_{solid}\,\rho_{ds}}{df^2} \cdot \left(\epsilon_{bw,n}^t \cdot \frac{\rho_{bw}}{\epsilon_{ds}\,\rho_{ds}} - R_{f,skin}(\varphi)\right)$

③ $\rho c_p\left(\frac{T_i^{t+1} - T_i^t}{\Delta t}\right) = k_{eff}\left(\frac{T_{n+1}^t - 2T_n^t + T_{n-1}^t}{\Delta x^2}\right) - (h_{sl}(\varphi) + \Delta h_{vap}(T))$
$(\dots) \cdot (\dot{m}$

→ resolve for k_{eff}, φ, D_{eff}.
→ move to next timestep.

Section 3: Node "n" (end)

Preamble

- $\varphi_n \cdot P_{sat}(T_n) = P_{vn, x=n\Delta x, t=0}$
- $P_g - P_{vo}(x = n\Delta x, t=0) = P_{a,}(x = n\Delta x, t=0)$
- $\epsilon_{g}(x = n\Delta x, t=0) = 1 - \epsilon_{ds} - \epsilon_{bw}$
- $h_m = \frac{h_{conv}}{\rho_a \cdot c_{p,a} \cdot Le^{2/3}}$

① $\epsilon_g\left(\frac{P_n^{t+1} - P_n^t}{\Delta t}\right) = D_{eff}\left(\frac{P_n - P_{n-1}}{\Delta x^2}\right) - h_m\left(\rho_{vair} - \rho_{vn}\right)$

② no bound water on surface

③ $\rho c_p\left(\frac{T_i^{t+1} - T_i^t}{\Delta t}\right) = k_{eff}\left(\frac{T_n - T_{n-1}}{\Delta x^2}\right) - h_c^{conv}(T_{amb} - T_i)$

Transient Solution for Sweating Mechanism on Fiber Volume

Contents

Part 0: Vanguard Mars Suit - 2018

The following code develops all the necessary equation required for calculating the time bound conditions for the heat and mass transfer equations involved in evaporative cooling of a skin surface due to multiple materials. The equations will be solved using a finite difference scheme. A Crank Nicolson approach to solving the PDE will be employed for the code. The code relies heavily on the works of the 3 major contributors: *(See Following)*

1. Gibson PW (1996) Multiphase heat and mass transfer through hygroscopic porous media with applications to clothing materials. Technical report Natick/TR-97/005.
2. P. Chitrphiromsri, and A.V. Kuznetsov (2005). Modeling Heat and Moisture Transport in Firefighter Protective Clothing during Flash Fire Exposure. Heat Mass Transfer, 41: 206-215, 2005.
3. S.F. Neves, J.B.L.M. Campos, T.S. Mayor (2017). Effects of clothing and fibres properties on the heat and mass transport, for different body heat/sweat releases, 117: 109-121, 2017.


```
%//% Begining of Code %//%
close all; clear; clc
```

Part 1: User Driven Input Conditions

Top level user will need to adjust the input conditions for the required material characteristics, ambient boundary condition, and skin surface condition. Furthermore, time bound info will also need to be added

1 Specify the Number of Nodes Needed for a 2 Layer Fabric Component

In this senario we are using fabric A for its ability to remove water, and fabric B for its ability to transfer heat out of the control volume. We assumed that this mechanism would be most optimal.

```
NodesA = 10 ;                       % Number of Nodes for Fabric A :
NodesB = 10;                        % Number of Nodes for Fabric B :
timeStp = 30;                       % (s) timestep
tTOtal  = 1800;                     % (s) Total Run time
totalStep = round(tTOtal/timeStp);  % Number of Iterations Needed

%//% Liquid-Cooling Garment (or lack of Garment) %//%
coolingfactor = 200;      % W/m^2 (200 W/m^2 is the normal effect)
```

Part 2 Strict Constants

```
%Total Pressure in ventillation compartment
P_Gmb = 31000;              % (Pa)
Temp_out = 20;              % (DegC)

% Air Constants
Ra = 287.058;               % j/(Kg-K) Air Gas Constant
Air_u = .5;                 % (m/s) Air Velocity in the outer medium
ka = 0.02596;               % (W/mK) Thermal Conductivity
Humidity_out = 50/100;      % (Humidity in percent
Ma = 28.97;
cpA = 1003;

% Water Vapor
Rv = 461.495;               % j/(Kg-K) Water Vapor Gas Constant
kv = 2.46E-2;               % (W/K-m) Thermal Conductivitiy of Saturated Water
cpV = 1862;                 % (J/ kg-K) Specific Heat

% Volume fraction of the water dissolved in the solid phase
Ebw0 = 0.01;                % Assume 0.1% initally

% Liquid Water
Mv = 18.01528;              % (g/mol) Molar Weight of Water
Kw = 0.609;                 % (W/m-K)  Thermal Conductivitiy of Water
rho_w = 1000;               % (kg/m3) Denity of Water
cpW = 4190;                 % (J/ kg-K)
%%%'
% *Moisture Absorbing Fabric Layer*
% The first layer is meant to wick up as much water from the skin as
% possible. We will have a larger diffusivity
```

```
%
Dsolid_fab1 = 4.5E-5;       % (m/s) Effective diffusivity of bound water
df1 = 1;                    % (m) Square diameter of fibre thread
Tau_fab1 =  2.49;           % (-) is the fabric tortuosity
rho_ds_fab1 = 250;          % (kg/m^3) Density of Fabric
Len_f1 = 0.850*10^(-3);     % (m) thickness of Fabric
Eds_f1 = 0.269;             % (-) volume fraction of the dry solid fiber
Regain_f1 = 0.056;          % (-)fabric regain at 65% relative humidity.
kds_fab1 = 0.40;            % (W/m-K)Thermal conductivity of fabric 1
cpDS1 = 1360;               % j/(Kg-K) Specific Heat of Fabric 1
```

1. Thermal liner for Fabric Layer 2

```
Dsolid_fab2 = 2.69E-5;      % (m/s) Effective diffusivity of bound water
df2 = 1;                   % (m) Square diameter of fibre thread
Tau_fab2 =  1.82;             % (-) is the fabric tortuosity
rho_ds_fab2 = 220;            % (kg/m^3) Density of Fabric
Len_f2 = 0.950*10^(-3);       % (m) thickness of Fabric
Eds_f2 = 0.300;               % (-) volume fraction of the dry solid fiber
Regain_f2 = 0.041;            % (-)fabric regain at 65% relative humidity.
kds_fab2 = 0.48;              % (W/m-K)Thermal conductivity of fabric 2
cpDS2 = 1285;                 % j/(Kg-K) Specific Heat of Fabric 1


% Human Skin Layer
%Surface Temperaure of skin - USE 41NODE Man
Temp_skin = 35;         % (DegC)
%Diameter of hand
Skin_Diam = 0.3;                                    % (m)
% Rate of increase of the mass of Sweat Vapor per unit volume of the mixture
% The noral value of person sweating is assumed to 9 (g/m3-hr)
SweatRate1 = 240 *(1/(3600*1000)); % (kg/m3-s)
SweatRate2 = 9.0 *(1/(3600*1000)); % (kg/m3-s)

% Metabolic heat production (g/m3-hr)
heat_production1 = 300; %(W/m^2)
heat_production2 = 59; %(W/m^2)
qin = heat_production1;
q_lcg = coolingfactor;
```

Part 2: Initialize Nodes Valuation

```
%Build Nodes Properties
Len_tot = Len_f1 + Len_f2;
delX = Len_tot/(NodesA + NodesB);
len_matrix = 0:delX:Len_tot;
med_val = find(len_matrix == median(len_matrix));
itot = length(len_matrix);
```

Part 3 Mass Transfer Functions

1. Arden Buck Equation Function that relate the saturation vapor pressure to temperature for moist air. This assumes T degC > 0 ; Output in (Pa)

```
ps = @(T) 0.61121*exp((18.678 - (T/234.5))*(T/(257.14+T)));
```

2. Sutherland Equation Needed to calculate the viscosity of gas

```
b = 1.458*10^(-5);               %(kg/m-s-K^1/2) b constant for Air;
S = 110.4;                       %(K) S constant for Air;
dy_u = @(T) b*(T^(3/2))*(1/(T+S));% Calculate Dynamic Viscosity
km_u = @(T,den) dy_u(T)/den;     % Calculate Kinematic Viscosity
```

3. Nusselt Number Function Calculate Nusselt Number to help deterimine Convective heat transfer coefficeint

```
Nu_N = @(Re,Pr) ...
    0.3 + ((0.62*(Re^(1/2)) * (Pr^(1/3)))) / ((1+ (0.4/Pr))^(1/4))*...
    ((1+((Re/282000)^5/8))^(4/5));
```

4. Marrero, T.R & E.A Mason al Gasseous Diffuision Coeffeint for use 273 K < T < 373K Calculate water vapor- air Diffusion Coeffient

```
D_H20_Air = @(T,P) (1.97*10^(-5))*(101.325/P)*((T/256)^(1.685));
```

5. Gibson PW - Effective diffusivity of the gas phase in the fabric

```
%The diffusivity of the water vapor in the air, Da, is calculated_
Da = @(T) (2.23*10^(-5))*(T/273.15)^(1.75);
%The volume fraction of gas in the fiber (1 - bound water - dry solid)_
Vol_Frac_Gas = @(Vol_Frac_Fab,Vol_Frac_BW) 1 - Vol_Frac_Fab - Vol_Frac_BW;
```

```
%Effective diffusivity of the gas phase in the fabric from above constants
Deff = @(T,Vol_Frac_BW,Vol_Frac_Fab,Tau) (Da(T)*Vol_Frac_Gas(Vol_Frac_Fab,Vol_Frac_BW))/(Tau);
```

6. The mass flux of the vapor out of the fiber due to Sorption

```
%A. The total fiber regain
Rftotal = @(ebw,eds,rho_ds) (ebw*rho_w)/(eds*rho_ds);

%B. Rfskin is the equilibrium regain at the fiber surface
Rfskin = @(Regain_65,Humidity,eds,rho_ds)...
    0.578*(Regain_65)*Humidity*((1/(0.321 + Humidity)) + (1/(1.262 - Humidity)));

%The mass flux of the vapor out of the fiber due to Sorption is calculated
%as follows (kg/m3-s)
Dsolidfun = @(Dsolid,rho_ds,df) (Dsolid*rho_ds)/(df^2);
msv = @(Dsolid,df,rho_ds,ebw,eds,Regain_65,Humidity) Dsolidfun(Dsolid,rho_ds,df)*(Rftotal(ebw,eds,rho_ds)  - Rfskin(Regain_65,Humidity,eds,rho_ds));
```

Part 4 Initalization of Key Variables

```
%Fabric Vapor Pressure & Density
P_Fab = Humidity_out*ps(Temp_skin+273.15);      % (Pa)
rho_Fab = (P_Fab) /(Rv*(Temp_skin+273.15));     % (kg/m^3)

% Ambient Vapor Pressure & Density
P_Vamb = Humidity_out*ps(Temp_out+273.15);      % (Pa)
rho_Vamb = (P_Vamb) /(Rv*(Temp_out+273.15));    % (kg/m^3)

% Ambient Air Pressure & Air Density using Ideal Gas Law
P_Aamb = P_Gmb - P_Vamb;                         % (Pa)
rho_Aamb = P_Aamb /(Ra*(Temp_out+273.15));       % (kg/m^3)
```

Assume air is modeled under ideal conditions of 1 Bar. The following is tabulated data from Moran, Michael J. Introduction to Thermal Systems Engineering : Thermodynamics, Fluid Mechanics, and Heat Transfer. New York : Wiley, c2003

```
T_val  = [250, 300, 350];
vdyn   = [11.44E-6, 15.89E-6, 20.92E-6];
pr_val = [0.720, 0.707, 0.700];
difsty = [15.9E-6, 22.5E-6, 29.9E-6];
```

Calculate Dimensionless Numbers

```
Re = (Air_u*Skin_Diam)...                                   % Reynolds Number
    /(interp1(T_val,vdyn,Temp_out+273.15,'PCHIP'));
Pr = interp1(T_val,pr_val,Temp_out+273.15,'PCHIP');         % Prandtl Number

DiffAB = D_H2O_Air(Temp_out+273.15,P_Gmb);       % (m2/s)
Le = interp1(T_val,difsty,Temp_out+273.15,'PCHIP')/DiffAB;  % Lewis Number
Nu = Nu_N(Re,Pr);                                           % Nusselt Number

% Calculate Convective Coefficeint
% Part 1 Convective Heat Transfer coefficeint
HeatTrans_Coeff = Nu*ka/Skin_Diam ;                             % (W/m2-K) Nusselt Expression
Ca = P_Aamb/(Ra*Temp_out+273.15);                               % (kg/m63) Concentration using Ideal Gas
MassTrans_Coeff = HeatTrans_Coeff/ (rho_Aamb*Ca*(Le^(2/3)));    % (m^2/s) Lewis Expression
```

Part 5: Heat Transfer Functions

```
%Enthalpy of transition from bound water to the free liquid water state
%(J/(Kg)), Deg K
del_hl = @(Humidity) (1.95E-5)*(1-Humidity)*((1/(0.2+Humidity))+(1/(1.05-Humidity)));

%Molar enthalpy of vaporization Gibson PW (1996) equations
%(J/(Kg)), Deg K
del_HVap = @(T) 2.792E6 -160*T - 3.43*T^2;

% The Thermal Conductivity of the Solid Phase
Ksig = @(ebw,Kds,rho_ds,eds) (Kw*rho_w*ebw + Kds*rho_ds*eds)/(rho_w*ebw + rho_ds*eds);
% The Thermal Conductivity of the Gas Phase
ky = @(rho_v)(kv*rho_v + ka*rho_Aamb)/(rho_v + rho_Aamb);
% Effective Thermal Conductivity of the Fabric
Keff = @(ebw,Kds,rho_ds,eds,rho_v)...
    (ky(rho_v))*((1+(ebw + eds)*Ksig(ebw,Kds,rho_ds,eds) + ky(rho_v))...
    /(Vol_Frac_Gas(eds,ebw)*Ksig(ebw,Kds,rho_ds,eds) + (1 + ebw + eds)*ky(rho_v)));

% Effective density of the fabric
Total_rho = @(ebw,rho_bw, eds, rho_ds, ey, rho_v, rho_a)...
    ebw*rho_bw + eds*(rho_ds) + ey*(rho_v+rho_a);

% Effective specific heat of the fabric
Cp_val = @(dens, ebw,rho_bw,cpw, eds,rho_ds,cpds, ey,rho_v,cpv, rho_a,cpa)...
    (ebw*(rho_bw)*cpw + eds*(rho_ds)*cpds + ey*(rho_v*cpv + rho_a*cpa))/dens;
```

Inital Condition Matrix

Remains Constant every time step

```
Fabric_VolFrac = [Eds_f1*(ones(med_val-1,1));...
                  .5*(Eds_f1+ Eds_f2);...
                  Eds_f2*ones(med_val-1,1)];

Fabric_Tau = [Tau_fab1*(ones(med_val-1,1));...
                  .5*(Tau_fab1+ Tau_fab2);...
                  Tau_fab2*ones(med_val-1,1)];

Fabric_rho_ds = [rho_ds_fab1*(ones(med_val-1,1));...
                  .5*(rho_ds_fab1 + rho_ds_fab2);...
                  rho_ds_fab1*ones(med_val-1,1)];
Fabric_cp_ds = [cpDS1*(ones(med_val-1,1));...
                  .5*(cpDS1 + cpDS2);...
                  cpDS2*ones(med_val-1,1)];

Fabric_k_ds = [kds_fab1*(ones(med_val-1,1));...
                  .5*(kds_fab1 + kds_fab2);...
                  kds_fab2*ones(med_val-1,1)];
```

Constants for Mass Transfer

Effective Density of the fabric Changes Every Time step

```
t = totalStep;
Fabric_rho_vapor = [rho_Fab*ones(itot,1),nan(itot,t)];                % (kg/m^3)
Fabric_rho_air = [((P_Gmb - P_Fab)/(Ra*(Temp_skin+273.15)))*ones(itot,1),nan(itot,t)]; %
Fabric_Humidity = [Humidity_out*ones(itot,1),nan(itot,t)];    % x Percent
BoundWater_Volfrac = [Ebw0*ones(itot,1),nan(itot,t)];         % Ebw
Gas_Volfrac = nan(itot,t+1);                                  % Ey
% Keff is the effective thermal conductivity of Fabric
Eff_KVal = nan(itot,t+1);
for i = 1: itot
Gas_Volfrac(i,1) = Vol_Frac_Gas(Fabric_VolFrac(i,1),BoundWater_Volfrac(i,1));
Eff_KVal(i,1) = Keff(BoundWater_Volfrac(i,1),Fabric_k_ds (i,1),...
            Fabric_rho_ds(i,1),Gas_Volfrac(i,1),Fabric_rho_vapor(i,1));
end

Eff_diff = nan(itot,t+1); % Deff Value

%mass flux of the vapor
mass_flux = nan(itot,t+1); % Deff Value

% Effective Density of the fabric
Eff_Dens = nan(itot,t+1);

% Effective specific heat of the fabric
Eff_Cp_Val = nan(itot,t+1);



Enthalp = nan(itot,t+1);
```

Part 6: Steady State Approximation of initial condition

```
%Effective diffusivity coefficient of Air-Vapor through Fabric 1
DAB1 = Deff(Temp_out+273,Ebw0,Eds_f1,Tau_fab1);
%Mass flux of the vapor out of the fiber (kg/m-s)
m_dot1 = msv(Dsolid_fab1,df1,rho_ds_fab1,Ebw0,Eds_f1,Regain_f1,Humidity_out);

%Effective diffusivity coefficient of Air-Vapor through Fabric 2
DAB2 = Deff(Temp_out+273,Ebw0,Eds_f2,Tau_fab2);
%Mass flux of the vapor out of the fiber (kg/m-s)
m_dot2 = msv(Dsolid_fab2,df2,rho_ds_fab2,Ebw0,Eds_f2,Regain_f2,Humidity_out);

%Matrix to Store Values
A_rho_matrix = zeros(length(len_matrix),length(len_matrix));
B_rho_matrix = zeros(length(len_matrix),1);

% A constant perspiration rate of 9g/m3-hr (i.e. insensible perspiration)
SweatRate = 9 *(1/(3600*1000)); % (kg/m3-s)
% Inital Condition
A_rho_matrix(1,1:2) = [-1 , 1];
B_rho_matrix(1,1) = (SweatRate*(delX^2/DAB1));

% Boundary Condition
A_rho_matrix(end,end-1:end) = [1 , (-1 + MassTrans_Coeff*(delX^2/DAB2))];
B_rho_matrix(end,1) = MassTrans_Coeff*(delX^2/DAB2)*(rho_Vamb);

% Middle Condition
for i = 2:length(len_matrix)-1
    if i < med_val
```

```
        A_rho_matrix(i,i-1:i+1) = [1 , -2 , 1];
        B_rho_matrix(i,1) =  -(delX^2/DAB1)*m_dot1;
    elseif i == med_val
        A_rho_matrix(med_val,med_val-1:med_val+1) = [DAB1 , -(DAB1+DAB2) , DAB2];
        B_rho_matrix(med_val,1) = -(.5*(m_dot1+m_dot2))*(delX^2);
    elseif i > med_val
        A_rho_matrix(i,i-1:i+1) = [1 , -2 , 1];
        B_rho_matrix(i,1) = -(delX^2/DAB2)*m_dot2;
    end
end
```

Initial Fabric Density

```
%rho_fabricNodes = -A_rho_matrix\B_rho_matrix
rho_fabricNodes = rho_Vamb*ones(length(len_matrix),1);
```

Part 7 Finite Difference Method - Heat Tranfer

```
%Calculate Effective Thermal Conductivity of the Fabric at every node
Effective_K = zeros(length(rho_fabricNodes),1);
for i = 1:length(rho_fabricNodes)
    if i < med_val
        Effective_K(i,1) = Keff(Ebw0,kds_fab1,rho_ds_fab1,Eds_f1,rho_fabricNodes(i,1));
    elseif i > med_val
        Effective_K(i,1) = Keff(Ebw0,kds_fab2,rho_ds_fab2,Eds_f2,rho_fabricNodes(i,1));
    end
end

% The enthalpy of transition from the bound water to the free liquid water state
hl_val = del_hl(Humidity_out)*ones(length(rho_fabricNodes),1);
%delHVAP = del_HVap(101.325,100+273.15,P_Vamb,Temp_surf+273);
delHVAP = del_HVap(Temp_skin+273);

%Matrix to Store Values
A_Tempmatrix = zeros(length(len_matrix),length(len_matrix));
B_Tempmatrix = zeros(length(len_matrix),1);

% Inital Condition
A_Tempmatrix(1,1) = 1;
B_Tempmatrix(1,1) = Temp_skin+273;

% Boundary Condition
A_Tempmatrix(end,end-1:end) = [1 , (-1 + HeatTrans_Coeff*(delX^2/Effective_K(end,1)))];
B_Tempmatrix(end,1) = HeatTrans_Coeff*(delX^2/Effective_K(end,1))*(Temp_out+273);

% Middle Condition
for i = 2:length(len_matrix)-1
    if i < med_val
        A_Tempmatrix(i,i-1:i+1) = [1 , -2 , 1];
        B_Tempmatrix(i,1) =  (delX^2/Effective_K(i,1))*(m_dot1)*(hl_val(i,1) +delHVAP);
    elseif i == med_val
        A_Tempmatrix(med_val,med_val-1:med_val+1) = [Effective_K(i-1,1) , -(Effective_K(i-1,1) + Effective_K(i+1,1)), Effective_K(i+1,1)];
        B_Tempmatrix(med_val,1) =  .5*(delX^2)*(m_dot1+m_dot2)*(hl_val(1,1) +delHVAP);
    elseif i > med_val
        A_Tempmatrix(i,i-1:i+1) = [1 , -2 , 1];
        B_Tempmatrix(i,1) =  (delX^2/Effective_K(i,1))*(m_dot1)*(hl_val(i,1) +delHVAP);
    end
end
```

Initial Fabric Temperature

```
temp_InitNodes = A_Tempmatrix\B_Tempmatrix;
Fabric_temp = [temp_InitNodes,nan(itot,t)];
NRG_nodes = zeros(itot,t);

A_rho_matrix = zeros(length(len_matrix),length(len_matrix));
B_rho_matrix = zeros(length(len_matrix),1);

A_temp_matrix = zeros(length(len_matrix),length(len_matrix));
B_temp_matrix = zeros(length(len_matrix),1);
for t = 1: totalStep
%%%%% Section 1 : Calculate Bound Water using Solid phase continuity equation %%%%%
%%%%% Finite Difference Method - Mass Tranfer - Section 1&2 %%%%%

    for i = 1: itot
        if i < med_val
            mass_flux(i,t) = abs(msv(Dsolid_fab1,df1,Fabric_rho_ds(i,1),BoundWater_Volfrac(i,t),Eds_f1,Regain_f1,Fabric_Humidity(i,t)));
        elseif i > med_val
            mass_flux(i,t) = abs(msv(Dsolid_fab2,df2,Fabric_rho_ds(i,1),BoundWater_Volfrac(i,t),Eds_f2,Regain_f2,Fabric_Humidity(i,t)));
        end

    end
        mass_flux(med_val,t) = abs(0.5*(mass_flux(med_val-1,t) + mass_flux(med_val+1,t))) ;

    for i = 1:itot
        BoundWater_Volfrac(i,t+1) = timeStp*((mass_flux(i,t)/rho_w))...
```

```
                                    + BoundWater_Volfrac(i,t);
        Gas_Volfrac(i,t+1) = Vol_Frac_Gas(Fabric_VolFrac(i,1),BoundWater_Volfrac(i,t+1));
    end

%%%%% Section 2 : Calculate Gas Phase Diffusivity equation - "rho"  %%%%%
    for i = 1: itot
        Eff_diff(i,t) = Deff(Fabric_temp(i,t),BoundWater_Volfrac(i,t),Fabric_VolFrac(i,1),Fabric_Tau(i,1));
    end

    % Initial Condition
    B1 = (2*Gas_Volfrac(1,t))/timeStp;
    B2 = Eff_diff(1,t)/delX^2;
    A_rho_matrix(1,1:2) = [(B1-B2) , (B2)];
    B_rho_matrix(1,1) = (B1 + B2)*Fabric_rho_vapor(1,t) ...        % Effect of time condition to vapor
                - B2*Fabric_rho_vapor(2,t) ...                     % Effect of losing vapor to adjacent
                + 2*(mass_flux(1,t)) + 2*SweatRate1;       % Effects of adding Vapor due to Perspiration


    % Boundary Condition
    B1 = (2*Gas_Volfrac(end,t))/timeStp;
    B2 = Eff_diff(end,t)/delX^2;
    A_rho_matrix(end,end-1:end) = [B2  , (B1-B2)];
    B_rho_matrix(end,1) = (-B2)*Fabric_rho_vapor(end-1,t) ...      % Effect of losing vapor to adjacent
      + (B1+B2)*(Fabric_rho_vapor(end,t))...                       % Effect of time condition to vapor
      + 2*MassTrans_Coeff*(rho_Aamb - Fabric_rho_vapor(end,t));...  % Effect of losing vapor to air



    % Middle Condition
    for i = 2:length(len_matrix)-1
        if i ~= med_val
            B1 = (2*Gas_Volfrac(i,t))/timeStp;
            B2 = Eff_diff(i,t)/delX^2;
            A_rho_matrix(i,i-1:i+1) = [B2 , (B1 - 2*B2) , B2];
            B_rho_matrix(i,1) = -B2*(Fabric_rho_vapor(i+1,t)...
                - 2*Fabric_rho_vapor(i,t) + Fabric_rho_vapor(i-1,t))... % Effect of losing vapor to diffusion
                + B1*Fabric_rho_vapor(i,t) ...                          % Effect of comparing vapor temporal
                + 2*mass_flux(end,t);                                   % Effects of adding Vapor due to Sorption
        else
            B1 = (2*Gas_Volfrac(i,t))/timeStp;
            B2 = Eff_diff(i,t)/delX^2;
            A_rho_matrix(i,i-1:i+1) = [B2 , (B1 - 2*B2) , B2];
            B_rho_matrix(i,1) = -B2*(Fabric_rho_vapor(i+1,t)...
                - 2*Fabric_rho_vapor(i,t) + Fabric_rho_vapor(i-1,t))... % Effect of losing vapor to diffusion
                + B1*Fabric_rho_vapor(i,t) + 2*mass_flux(i,t) ;                        % Effect of comparing vapor temporal

        end
    end

    Fabric_rho_vapor(:,t+1) = (A_rho_matrix\B_rho_matrix);
 %%%%% Section 3 : Calculate Temperature using the Energy equation  %%%%%
 % Build required constants
    for i = 1: itot
        % Density_t
        Eff_Dens(i,t) = Total_rho(BoundWater_Volfrac(i,t),rho_w, ...
                    Fabric_VolFrac(i,1), Fabric_rho_ds(i,1), ...
            Gas_Volfrac(i,t), Fabric_rho_vapor(i,t), Fabric_rho_air(i,t));
        % Cp_t
        Eff_Cp_Val(i,t) = Cp_val(Eff_Dens(i,t),BoundWater_Volfrac(i,t),rho_w,cpW, ...
                    Fabric_VolFrac(i,1), Fabric_rho_ds(i,1), Fabric_cp_ds(i,1), ...
                    Gas_Volfrac(i,t), Fabric_rho_vapor(i,t),cpV,...
                    Fabric_rho_air(i,t), cpA);
        % Keff_t+1 & Keff_t
        Eff_KVal(i,t+1) = Keff(BoundWater_Volfrac(i,t+1),Fabric_k_ds (i,1),...
            Fabric_rho_ds(i,1),Gas_Volfrac(i,t+1),Fabric_rho_vapor(i,t+1));
        % (delHL + delHVap)
        Enthalp(i,t) = (del_hl(Fabric_Humidity(i,t)) + del_HVap(Fabric_temp(i,t)));
    end
% Initial Condition
    B1 = (2/timeStp)*Eff_Dens(1,t)*Eff_Cp_Val(1,t);
    B2 = Eff_KVal(1,t)/delX^2;
    B3 = Eff_KVal(1,t)/delX^2;
    A_temp_matrix(1,1:2) = [(B1 - B2) , B2];
    B_temp_matrix(1,t) = (B1 + B3)*Fabric_temp(1,t)...          % Temporal Effect of Temperature change
                        - B3*Fabric_temp(2,t)...                % Temporal Effect of Temperature change
                        - 2*mass_flux(1,t)*(Enthalp(1,t))...
                        + 2*qin*(1/delX);                                  %Effects of adding Vapor due to Perspiration
    NRG_nodes(1,t) =  -2*mass_flux(1,t)*(Enthalp(1,t));

    % Boundary Condition
    B1 = (2/timeStp)*Eff_Dens(end,t)*Eff_Cp_Val(end,t);
    B2 = Eff_KVal(end,t)/delX^2;
    B3 = Eff_KVal(end,t)/delX^2;
    A_temp_matrix(end,end-1:end) = [B2  , (B1-B2)];
    B_temp_matrix(end,t) = (-B3)*Fabric_temp(end-1,t) ...
                         + (B1+B3)*(Fabric_temp(end-1,t))...
                         - 2*HeatTrans_Coeff*(Fabric_temp(end,t)-(Temp_out+273))*(1/delX)...
                         - 2*mass_flux(end,t)*(Enthalp(end,t))...
                         - q_lcg*(1/delX);
    NRG_nodes(end,t) = -2*HeatTrans_Coeff*(Fabric_temp(end,t)-(Temp_out+273))*(1/delX)...
```

```
        - 2*q_lcg*(1/delX);

    % Middle Condition
    for i = 2:length(len_matrix)-1
        if i ~= med_val
            B1 = (2/timeStp)*Eff_Dens(i,t)*Eff_Cp_Val(i,t);
            B2 = Eff_KVal(i,t)/delX^2;
            B3 = Eff_KVal(i,t)/delX^2;
            A_temp_matrix(i,i-1:i+1) = [B2 , (B1 - 2*B2) , B2];
            B_temp_matrix(i,t) = -B3*(Fabric_temp(i+1,t)...
                - 2*Fabric_temp(i,t) + Fabric_temp(i-1,t))... % Effect of losing vapor to diffusion
                + B1*Fabric_temp(i,t) ...                     % Effect of comparing vapor temporal
                - 2*mass_flux(1,1)*(Enthalp(end,1));                                    % Effects of adding Vapor due to Sorption
                NRG_nodes(i,t) =  -2*mass_flux(1,1)*(Enthalp(end,1));
        else
            B1 = (2/timeStp)*Eff_Dens(i,t)*Eff_Cp_Val(i,t);
            B2 = Eff_KVal(i,t)/delX^2;
            B3 = Eff_KVal(i,t)/delX^2;
            A_temp_matrix(i,i-1:i+1) = [B2 , (B1 - 2*B2) , B2];
            B_temp_matrix(i,t) = -B3*(Fabric_temp(i+1,t)...
                - 2*Fabric_temp(i,t) + Fabric_temp(i-1,t))... % Effect of losing vapor to diffusion
                + B1*Fabric_temp(i,t) ...                     % Effect of comparing vapor temporal
                - 2*mass_flux(1,t)*(Enthalp(end,1));                                    % Effects of adding Vapor due to Sorption
                NRG_nodes(i,t) =  - 2*mass_flux(1,1)*(Enthalp(end,1));
        end
    end
    Fabric_temp(:,t+1) = (A_temp_matrix\ B_temp_matrix(:,t));

     for i = 1:itot
      Pnew_Fab = Fabric_rho_vapor(i,t+1)*(Rv*(Fabric_temp(i,t+1)));
      Fabric_Humidity(i,t+1) = Pnew_Fab/ps(Fabric_temp(i,t+1));
      Fabric_rho_air(i,t+1) = (P_Gmb - Pnew_Fab)/(Ra*(Fabric_temp(i,t+1)));

     end

end
% figure(1)
%     subplot(2,1,1);
%     plot(len_matrix,Fabric_rho_vapor(:,1),'LineWidth' , 3)
%     hold on
%     plot(len_matrix,Fabric_rho_vapor(:,t+1),'LineWidth' , 3)
%     title ('Water Vapor Density');
%     xlabel({'Fabric Length', '(m)'})
%     ylabel({'Density', '(kg/m3)'})
%     legend({'Time = 0 min', 'With LCG'},'Location','east')
%     set(gca,'fontsize',10)
%
%
%     subplot(2,1,2);
%     plot(len_matrix,Fabric_temp(:,1),'LineWidth' , 3)
%     hold on
%     plot(len_matrix,Fabric_temp(:,t+1),'LineWidth' , 3)
%     title ('Fabric Temperature Distribution');
%     xlabel({'Fabric Length', '(m)'})
%     ylabel({'Temperature', '(K)'})
%     legend({'Time = 0 min', 'With LCG'},'Location','east')
%     set(gca,'fontsize',10)
%


% %% Plot Results
% x = nan(1,totalStep);
% y = nan(1,totalStep);
% ydata_s = nan(1,totalStep);
%  for t = 1:totalStep
%      x(t) = (t-1)*timeStp*(1/60);
%      y(t) = mean(Fabric_temp(1:itot,t));
%      ydata_s(t)  = std(Fabric_temp(1:itot,t));
%  end
% figure
% hold on
% hA = plot(x,y);
% hE =  errorbar(x,y,ydata_s);
% set(hA                          , ...
%   'LineWidth'       , 2         , ...
%   'Color'           , [0 0 .5]    );
%
% set(hE                          , ...
%   'LineWidth'       , 1         , ...
%   'Marker'          , 'o'       , ...
%   'MarkerSize'      , 6         , ...
%   'MarkerEdgeColor' , [.2 .2 .2]  , ...
%   'MarkerFaceColor' , [.7 .7 .7]  , ...
%   'Color'           , [.3 .3 .3]  );
% hTitle  = title ('Average Temperature in Clothing - Time Bound');
% hXLabel = xlabel({'Time', '(Minutes)'}                                  );
% hYLabel = ylabel({'Temperature', '(degrees K)'}                         );
% set(gca,'fontsize',20)
% hLegend = legend(                                          ...
%                   [hE, hA,], ...
```

```
%                'Averaged Data points' , ...
%                'Fit'                                          );
%
% hold off
%
% figure
%  for t = 1:totalStep
%      x(t) = (t-1)*timeStp*(1/60);
%      y(t) = 1*sum(NRG_nodes(:,t))*delX;
%  end
% y2 = mean(y)*ones(1,t);
% y3 = std(y(5:end));
% plot(x, y, 'LineWidth', 0.5)
% s = num2str(y2(1));s2 = '\uparrow The average power lost from the system is:';
% txt3 = strcat(s2,{' '},s,{' '},'Watts');
% text(x(end-1),1.05*(y2(1)-y3(1)),txt3,'HorizontalAlignment','right')
% line(x, y2, 'Color', 'k', 'LineStyle', '-', 'LineWidth', 2)
% line(x, y2+y3, 'Color', 'r', 'LineStyle', '--', 'LineWidth', 2)
% line(x, y2-y3, 'Color', 'r', 'LineStyle', '--', 'LineWidth', 2)
% legend({'Data', 'Average', 'Std Deviation'},'Location','Southeast');
% title ('Average Power lost from the system');
% xlabel({'Time', '(Minutes)'});
% ylabel({'Power', '(Watts)'});
% set(gca,'fontsize',20)
```

Published with MATLAB® R2017b